A Systematic Study of Film Formation in CO_2 Corrosion

by

Nur Aisah Binti Zakaria

Dissertation submitted in partial fulfilment of
The requirements for the
Bachelor of Engineering (Hons)
(Mechanical Engineering)

AUGUST 2011

Universiti Teknologi PETRONAS
Bandar Seri Iskandar
31750 Tronoh
Perak Darul Ridzuan

CERTIFICATION OF APPROVAL

A Systematic Study of Film Formation in CO_2 Corrosion

by

Nur Aisah Binti Zakaria

A project dissertation submitted to the
Mechanical Engineering Programme
Universiti Teknologi PETRONAS
in partial fulfilment of the requirement for the
BACHELOR OF ENGINEERING (Hons)
(MECHANICAL ENGINEERING)

Approved by,

Assoc. Prof. Ir. Dr. Mokhtar Che Ismail

UNIVERSITI TEKNOLOGI PETRONAS

TRONOH, PERAK

August 2011

CERTIFICATION OF ORIGINALITY

This is to certify that I am responsible for the work submitted in this project, that the original work is my own except as specified in the references and acknowledgements, and that the original work contained herein have not been undertaken or done by unspecified sources or persons.

NUR AISAH BINTI ZAKARIA

ABSTRACT

CO_2 corrosion is one of the major problems in oil and gas industry. The formation of $FeCO_3$ film in CO_2 corrosion is observed to provide corrosion protection; however, the degree of protection is unclear. The main objective of this study is to understand the mechanism of protective film formation in CO_2 environment with the aim to assess the potential as corrosion mitigation and possible interaction between corrosion inhibitor and film formation. The film formation tests were conducted in one-litre glass cell under typical CO_2 corrosion test set-up by two film formation methods - natural film and induced film formation with 50 and 100ppm Fe^{2+} ions .The interaction of corrosion inhibitor and induced $FeCO_3$ film fromation were studied for two cases; full protection of corrosion inhibitor dosage of 50ppm and partial protection at 25ppm corrosion inhibitor. Both studies were done at pH 6.0 and for 24 hours of immersion. Corrosion rates were measured electrochemically by Electrochemical Impedance Spectroscopy (EIS), Linear Polarization Resistance (LPR). The condition of the film formation was analyzed by both Scanning Electron Microscopy (SEM) and EIS.

The result s showed that for the natural film formation, the corrosion rate at 80°C was lower than at 50°C which were 0.34 mm/year and 1.78 mm/year respectively. Same trend of corrosion rate obtained from induced film formation where at 80°C, the corrosion rate was 0.98 mm/year and at 50°C the corrosion rate was 0.04 mm/year. With high concentration of corrosion inhibitor deployment, the corrosion rate was low. By injecting 50ppm imidazoline, the corrosion rate was 0.03 mm/year and at 25ppm imidazoline, the corrosion rate was 0.76 mm/year. Interaction of $FeCO_3$ and imidazoline was possible where by induced 50ppm and 100ppm of Fe^{2+}, the corrosion rate were at 0.06 mm/year and 0.02 mm/year respectively.

$FeCO_3$ film formation in CO_2 corrosion is due to solubility of $FeCO_3$ which depends on functions like saturation, pH and temperature. Partial $FeCO_3$ formation as produced at 80 °C under natural film formation reduces corrosion rate to 0.34 mm/year. Protective film formation as produced for inducing method reduces corrosion rate down to 0.04 mm/year. This proves that protective film could reduce the corrosion rate and method to accelerate film formation could be beneficial to mitigate corrosion.

The mechanism of corrosion inhibitor adsorption is different than $FeCO_3$ film formation. Corrosion inhibitor with sufficient dosage will be able to reduce corrosion rate to a low value and $FeCO_3$ film was not formed. A possible positive interaction between corrosion inhibitor and $FeCO_3$ formation could occur whereby low corrosion inhibitor dosage will be supplemented by the formation of $FeCO_3$ film to reduce the corrosion rate to a low value.

ACKNOWLEDGEMENT

In the name of Allah, The Most Merciful and Most Compassionate

Heartiest gratitude to Assoc. Prof. Ir. Dr. Mokhtar Che Ismail, the supervisor of this project, for his invaluable guidance and encouragement extended throughout the study. His continuous supervision, suggestion, patience and guidance deserve a special mention.

Earnest thanks go to Ms. Sarini Bt. Mat Yaakob, Mr. Martin Choirul Fatah and Dr. Yuli Panca Asmara for their co-operation, thoughts and idea in helping me to understand the projects, prepare samples and support along the way to complete the project. Besides that, special thanks to Mechanical Laboratory technicians, particularly to Mr M. Faisal Ismail, Mr. Irwan Othman and Mr. Paris for their help and assistance during laboratory works.

In addition, the author would like to thank her fellow colleagues for their constructive comments and knowledge sharing during the progress of this project. Not forgetting the author's beloved parents, Mr. Zakaria Bin Yeop Ahmad and Madam Rakiah Binti Shoib and entire family, the author would like to express sincere gratitude for their never ending encouragement along the way.

Lastly, the author would like to thank all who have contributed in any way, directly or indirectly in the process of carrying out the project.

LIST OF FIGURES

LIST OF TABLES

TABLE OF CONTENTS

CHAPTER 1
INTRODUCTION

1.1 Background Study

Corrosion refers to the undesirable deterioration of a metal due to the interaction of the metal with environment. CO_2 corrosion is a main corrosion threat in oil and gas industry. The selection of construction material is influenced by CO_2 corrosion.

Carbon steel is a primary construction material for oil and gas pipelines but susceptible to corrosion in CO_2 environment. The motivation to use carbon steel as construction material is influenced by economical factor. As such, the utilization of carbon steel is usually combined with corrosion control method such as corrosion allowance and corrosion inhibitor injection. Furthermore, the formation of $FeCO_3$ film on the surface under certain conditions and can prevent the metal from further corrosion by acting as a diffusion barrier.

From previous researches and studies, it is known that the $FeCO_3$ film formation provides some corrosion protection as it acts as diffusion barrier for any further corrosion attack. Once protective film is formed, the rate of corrosion of corrosion can be reduced substantially. Therefore, to gain more understanding of the kinetics and the effectiveness of the film, LPR and EIS technique have been used to characterize of the film.

However, the reliance on the $FeCO_3$ film is questionable and not widely accepted. This is partly due to unclear mechanism of the film formation in CO_2 environment and also the interaction of the film with corrosion inhibitor.

On the other hand, pH neutralization technique proposed by the IFE, capitalizes on the idea of protection $FeCO_3$ film at higher pH. Thus, the understanding of the film formation is beneficial as this could provide additional protection to the carbon steel pipeline. The mechanism study of the $FeCO_3$ the film formation depends on the kinetics of the process.

By using Electrochemical Impedance Spectroscopy (EIS), the formation of $FeCO_3$ film layer can be predicted. The prediction can be evaluated by focusing on formation of multiple layers of $FeCO_3$ if Fe^{2+} ions have been induced. This is important to determine the layer is protective, semi-protective and not protective. Significantly, a better material selection process could be done in the oil and gas industry.

The analysis of the mechanism of film formation in CO_2 corrosion is necessary to generate more understanding, thus provide useful information in predicting the formation of protective corrosion product. Therefore, it will facilitate us to design a reliable and cost effective technique in oil and gas industry.

1.2 Problem Statement

Corrosion control of carbon steel CO_2 corrosion always depends on the corrosion allowance and corrosion inhibitors deployment. However, the control strategy assumes no interaction with $FeCO_3$ film formation. As such, there is no clear understanding of the interaction between the corrosion inhibitor and $FeCO_3$ film.

1.3 Objectives

The objective of this study is to understand and analyze the formation of $FeCO_3$ film in CO_2 corrosion, specifically in terms of:

- the effect of $FeCO_3$ on corrosion rate in natural filming condition
- the effect of multiple layers of $FeCO_3$ and the corrosion rate by inducing film formation.
- the interaction between corrosion inhibitor and $FeCO_3$ by inducing film formation

CHAPTER 2
LITERATURE REVIEW

2.1 Overview of CO_2 Corrosion

CO_2 corrosion is one of the important concerns in oil and gas production and transportation industry [10]. The study of CO_2 corrosion rate and $FeCO_3$ film formation are essential to enhance the understanding and modelling the kinetics of $FeCO_3$ precipitation process.

The presence of CO_2 in solution would initiate the CO_2 corrosion process. It would produce a weak carbonic acid (H_2CO_3) as presented by equation (2.1) below:

$$CO_2 + H_2O \longrightarrow H_2CO_3 \qquad (2.1)$$

The reaction process will continue with three cathodic reactions (reduction) and one anodic reaction (oxidation). The cathodic reactions in CO_2 solutions are:

1. Reduction of carbonate acid into bicarbonate ions.
   $$2H_2CO_3 + 2e^- \longrightarrow H_2 + 2HCO_3^- \qquad (2.2a)$$

2. Reduction of bicarbonate ions into carbonate ions.
   $$2HCO_3^- + 2e^- \longrightarrow H_2 + 2CO_3^- \qquad (2.2b)$$

3. Reduction of hydrogen ions.
   $$2H^+ + 2e^- \longrightarrow H_2 \qquad (2.2c)$$

The CO_2 corrosion reaction includes the anodic dissolution of iron into ferrous ions at the metal surface and given by:

$$Fe \longrightarrow Fe^{2+} + 2e^- \qquad (2.3)$$

This corrosion reaction promotes the formation of $FeCO_3$ which can form along a couple of reaction paths. First, ferrous ions will react with bicarbonate ions to form $FeCO_3$ as given by:

$$Fe^{2+} + CO_3^{2-} \longrightarrow FeCO_3 \qquad (2.4)$$

$FeCO_3$ can also form by two processes. When ferrous ions react with bicarbonate ions, ferrous iron bicarbonate forms consequently dissociates into iron carbonate, carbon dioxide and water.

$$Fe^{2+} + 2HCO_3^- \longrightarrow Fe(HCO_3)_2 \qquad (2.5a)$$

$$Fe(HCO_3)_2 \longrightarrow FeCO_3 + CO_2 + H_2O \qquad (2.5b)$$

This overall reaction of CO_2 corrosion leads to the formation of $FeCO_3$. Precipitation of $FeCO_3$ could form a protective film on the metal surface and prevent the metal from further corrosive attack.

2.2 Factors Affecting CO_2 Corrosion

There are several important factors that would affect CO_2 corrosion. Eventually, from these factors the formation of protective corrosion product would also be affected, which affect the corrosion rate of metal. The parameters comprise pH, temperature, CO_2 partial pressure, Fe^{2+} concentration and fluid velocity.

2.2.1 pH

CO_2 corrosion involves three cathodic reactions, which are reduction of carbonic acid, reduction of bicarbonate ions and reduction of hydrogen ions. From research, change of pH in solution would affect or change the physical properties of iron carbonate and corrosion rate. With change of electrolyte pH, the concentration of dissolved species from reduction process such as HCO^{3-} ions, CO_3^{2-} ions and H^+ ions changes, therefore affect the rate of cathodic reaction.

Generally, the increasing of pH value in the solution increases the cathodic reaction and as a result, the solubility of Fe^{2+} and CO_2^{3-} is decreasing. This condition would make ease for these ions to reach and exceed the solubility limit and precipitate as iron carbonate [8]. Consequently, the corrosion rate would deplete because of increasing of protective iron carbonate on the metal surface.

2.2.2 Temperature

Temperature has an important role in formation of $FeCO_3$ film layer. As the temperature increase, the corrosion rate would increase as well until it reaches a critical temperature [3]. Above the critical temperature, the precipitation of $FeCO_3$ would begin and reduce the corrosion rate. Researchers have approves that the rate of corrosion can be controlled by either increasing the pH solution or increasing the temperature [6]. This indicates that there is interrelation between these factors that affects CO_2 corrosion.

Increasing the temperature actually can either increase or decrease the corrosion rate depending whether the solubility of $FeCO_3$ is exceeded or reaches the supersaturation. At low pH, the corrosion rate would increase accordingly with increasing temperature as the protective film does not form. At high pH, the precipitation rate of iron carbonate getting higher and this indicate that concentration of Fe^{2+} and CO_3^{2-} exceed the solubility limit, enables the formation of $FeCO_3$ hence resulting a lower corrosion rate.

2.2.3 CO_2 Partial Pressure

Generally, the solubility of gas in a liquid would always depend on the temperature, the partial pressure and the nature of solvent and gas as well. According to Henry's Law, the concentration of dissolved gas will always depends on the partial pressure of the gas as the partial pressure controls the number of collisions between the gas molecules with the surface of the solution [7].

For CO_2 corrosion, when there is a favourable condition which would be high temperature and pH, increasing the CO_2 partial pressure would increase the precipitation rate of $FeCO_3$ as the result of more concentration of Fe^{2+} and CO_3^{2-} dissolved hence reducing the corrosion rate. In the condition of low pH and temperature, the opposite effect occurs which increasing the concentration of H_2CO_3 in the solution.

2.2.4 Fe^{2+} Concentration

The formation rate of protective iron carbonate depends on the precipitation rate of Fe^{2+} and CO_3^{2-}. The precipitation would occur when the concentration of the required ions exceeds the solubility limit and reaches beyond supersaturation degree limit [7]. Given that to find the supersaturation of iron carbonate is by using equation below:

$$\text{Supersaturation} = \frac{c_{Fe^{2+}}\, c_{CO_3^{2-}}}{K_{sp}} \qquad (2.6)$$

K_{sp} is the solubility limit which the value can determine the ions activity in solution. Consequently, lower solubility limit would increase the supersaturation of $FeCO_3$. By increasing the concentration of Fe^{2+} by external sources and anodic reaction, it is easier for protective iron carbonate film to form and reducing the corrosion rate.

2.2.5 Flow Velocity

Increasing the flow velocity in the solution will result in higher rate of corrosion in CO_2 environment because there will be lower precipitation of $FeCO_3$. High flow velocity leads to reduction of surface saturation of Fe^{2+} and CO_3^{2-} on the metal surface since there is turbulence near the wall [1]. The situation prevents $FeCO_3$ precipitation to occur and increasing the corrosion rate.

2.3 $FeCO_3$ Film Formation

$FeCO_3$ formation is one of the most important factors governing the corrosion rate. It is eventually reduce the corrosion rate, dependant on several factors involved such as steel type, fluid flow velocity, temperature, CO_2 partial pressure, pH and Fe^{2+} concentration.

To form $FeCO_3$ films, concentration of $FeCO_3$ must exceed the solubility limit. For that reason, a very high saturation is needed to form the protective films and to obtain a successful protection. The precipitation of $FeCO_3$ is described as slow and temperature dependant process, the corrosion rate will increase accordingly until the protective iron carbonate is fully formed at the surface [9]. At higher temperature, the $FeCO_3$ solubility is reduced and the precipitation rate is much faster thus allowing the formation of iron carbonate films.

The formation of $FeCO_3$ depends primarily on the precipitation kinetics. To calculate the precipitation, two different expressions have been introduced to describe the kinetics of the $FeCO_3$ formation in CO_2 corrosion. The equations are given by:

$$PR = k_r \frac{A}{V} K_{sp}\{(SS)^{0.5} - 1\}^2 \quad (2.7a)$$

$$PR = k_r \frac{A}{V} K_{sp}(SS - 1)(1 - SS^{-1}) \quad (2.7b)$$

The equations above show that rate of precipitation, PR is the function of iron carbonate supersaturation, SS, the solubility K_{sp}, temperature and surface area-to-volume ratio A/V.

The supersaturation value of the solution should remain high to ensure the iron carbonate layer and is effective and efficient. Research done indicate that supersaturation plays an important role to enhance the precipitation rate of $FeCO_3$ formation thus reduce the corrosion rate [5].

Although the governing equations have been determined by researches, there should be further analysis as for the precipitation kinetics of $FeCO_3$ as there is much estimation and theories to determine the corrosion rate, thus prediction of the precipitation behaviour can be verified.

2.4 Effect of Corrosion Inhibitors to CO_2 Corrosion

Corrosion inhibitor is one of the methods for corrosion control which designed to protect a metal or alloy from corrosion. The molecules in inhibitor attached directly to the surface, normally only one molecular thick and do not penetrate into the bulk of the metal itself. For this test study, the corrosion inhibitors that will be used is imidazoline.

The previous researches have study how inhibitors which is imidazoline interact with $FeCO_3$. From the study, imidazoline inhibitor prevents the growth of $FeCO_3$ and act as scale inhibitors which could be due to the decrease of Fe^{2+} at the metal surface [2]. This situation also occurs as when there are pre-corrosion that actually more suit to the oil and gas filed. There are different types of scales during pre-corrosion but the most significant is the formation of iron carbide (Fe_3C) film which would leads to the increment of corrosion rate. The imidazoline interaction would be efficient for a concentration of 20 to 50 ppm to reduce the corrosion rate [4].

There are also study that the interaction between inhibitors and protective film is efficient when either the species alone. With varies concentration of inhibitors, the experiments has successfully indicate that neither species dominates the adsorbed film, however a synergistic relationship has occurred to decrease the corrosion effect [2].

2.5 Electrochemical Measurement Techniques

The test study would be analyzed by using EIS and LPR technique. These methods would provide the corrosion rate on the effect of the formation of $FeCO_3$ to the metal surface. The data and analysis obtained would offer a cost effective and reliable prediction on CO2 corrosion.

2.5.1 Electrochemical Impedance Spectroscopy (EIS)

EIS is a non-destructive technique to evaluate a wide range of materials. Also known as AC impedance spectroscopy, this method is broadly applied in corrosion as its role in analyzing the kinetic properties and mechanism. EIS provides solid information regarding the electrode surface and the interfacial properties with an electrically conducting electrode. The corrosion mechanisms and its properties can easily understand by knowing the basic electrochemical reactions at the electrode surface.

EIS is based on Ohm's Law that defines the ratio of voltage over current, represented by:

$$R = E/I \tag{2.8}$$

This relationship is limited to one circuit element, which is the resistor. However, in the real world of electrochemical process, it contains much more complex behaviour that actually can be modelled by various circuit elements such as capacitors and inductors. For that matter, it is easier to apply the electrochemical impedance technique as for its ability to model a corrosion process.

Electrochemical impedance is measured by applying small amplitude of sinusoidal excitation signal. In response for this potential is AC current signal. The current respond will be sinusoid at the same frequency but shifted in phase.

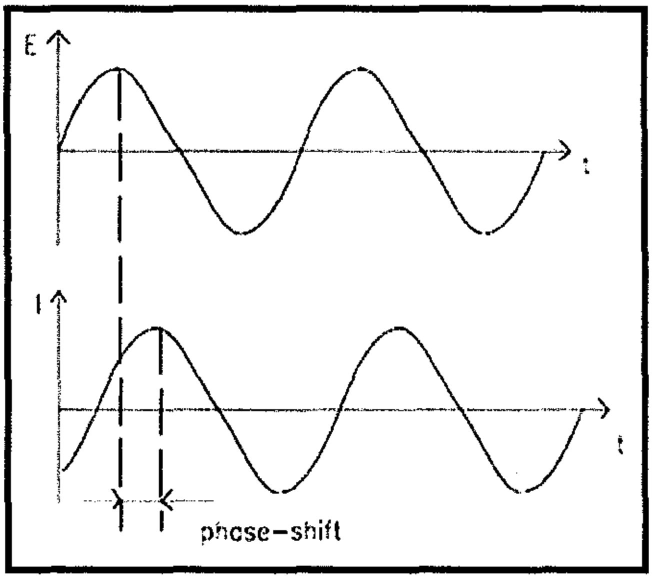

Figure 2.1: Sinusoidal Current Response in Linear System

The electrochemical impedance $Z(\omega)$, is the relationship between both excitation voltage signal and the current response in transfer function, shown in equation below:

$$Z(\omega) = E(\omega) / I(\omega) \qquad (2.9)$$

Data representation for $Z(\omega)$ is composed of real part (X-axis) against the imaginary part (Y-axis) to obtain a "Nyquist plot". In this plot, impedance can be represented as a vector of length $|Z|$ and the angle between the vector and X-axis is the phase angle.

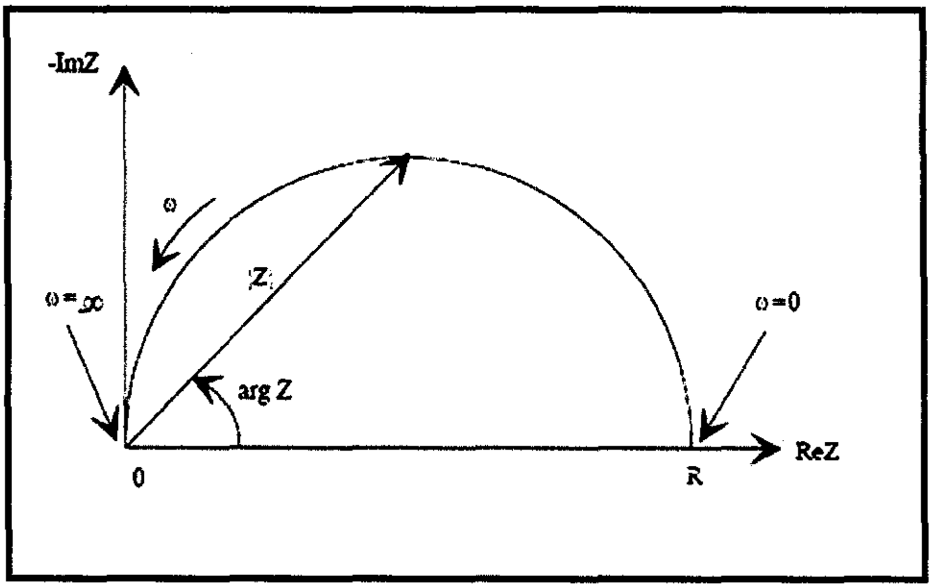

Figure 2.2: Nyquist Plot with Impedance Vector

The advantage of Nyquist plot is that it gives a quick overview of the data and can make some qualitative interpretations. However, this plot would be not indicate the frequency measurement of the data. To overcome this problem, a "Bode plot" was introduced where the impedance and phase shift ape plotted in two different plots.

Consequently, by getting the measurement of impedance Z, the corrosion mechanism information as well as the corrosion rate can be derived from the obtained values.

2.5.2 Linear Polarization Resistance (LPR)

LPR technique is been used for measuring the corrosion rate directly, in real time. The method generates a plot of current (I) versus potential over a small potential range. The polarizing voltage of 10mV has been chosen to obtain the linear relationship between I_{corr} and $\Delta E/\Delta I$. The value is sufficiently small as to cause no significant or permanent disruption of the corrosion process, so that the measurements would valid for the entire experiments.

The linear relationship was derived by Stern and Geary, and known as Stern-Geary equation, that relates the slope of the linear region to the Tafel slopes and corrosion current. [7]

$$R_p = \frac{b_a \cdot b_c}{2.303\,(b_a + b_c) \cdot i_{corr}} = \frac{\Delta E}{\Delta I} \qquad (2.10)$$

Where Rp is the polarization resistance, i_{corr} is the corrosion current b_a and b_c is the anodic and cathodic Tafel slopes respectively.

The slope of the linear relationship would gives the polarization resistance, R_p which it is inversely proportional to the uniform corrosion rate and can be applied to Stern – Geary equation to determine the corrosion current and corrosion rate.

CHAPTER 3
METHODOLOGY

3.1 Introduction

The laboratory experiments will be conducted by using X52 carbon steel with several condition to achieve the objectives which are to analyze the $FeCO_3$ film formation and its protectiveness towards metal surface. Once the results were obtained, the analysis continues by applying EIS technique as well as SEM to examine the film formation. The detail project flow and schedule can be referred to the Gantt chart (*Appendix 2*).

3.2 Sample Preparation

3.2.1 Planning

The laboratory experiments will be conducted by using X52 carbon steel (refer *Appendix 1* for the element composition). Next, the X52 will be manufactured in the lab to cut into small pieces, for the experiment purposes. Chemicals such as, CO_2 gas and sodium chloride (NaCl) solutions need to be purchased before carry out the experiments.

The sample preparation would be done accordingly by using steps shown in the figure:

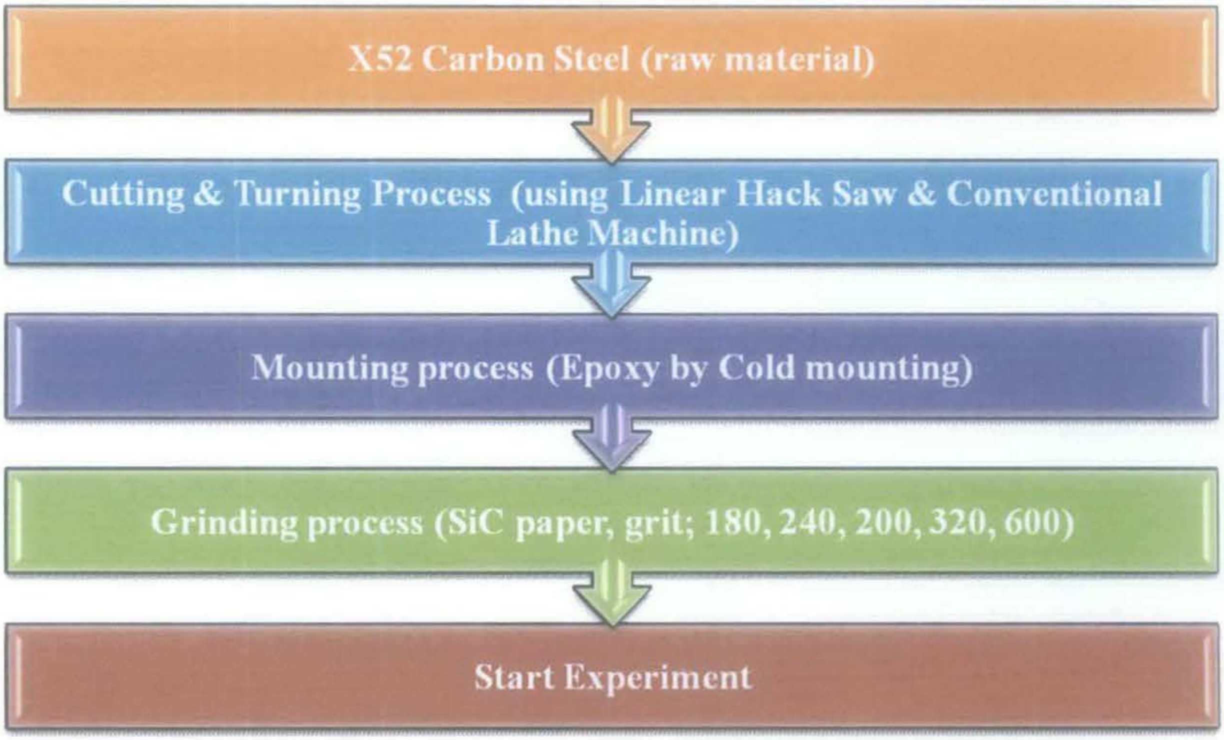

Figure 3.1: Step by step procedure for sample preparation

3.2.2 Works Done

The material required for all the experimental work would be X52 carbon steel that is a common material in oil and gas field. The material sample is first been through some process before can be utilized in the research.

In the beginning, X52 carbon steel has been cut to a rectangle and suitable pieces by using the linear hack saw machine.

Figure 3.2: Linear Hack Saw Machine

Next, the conventional lathe machine the sample has been manufactured into cylindrical shape with a diameter of 1.2cm. The process continues by cutting the sample accordingly with an appropriate thickness to set up the experimental work. There are also a square shape of specimens that has been cut into small pieces for the same purpose.

Figure 3.3: X52 Carbon Steel after undergoing turning process

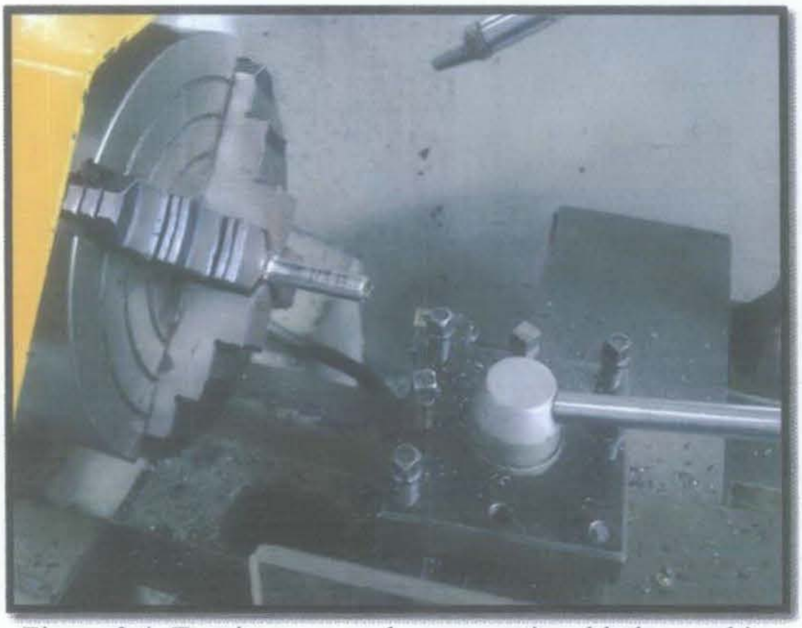

Figure 3.4: Turning process by conventional lathe machine

Next step is to mount the specimen by using epoxy and cold mount it for one day to ensure the mount is strong enough to hold the specimen. The purpose of specimen is to avoid any wear or damage to the specimen while doing the experiment. Besides that, the grinding process of specimen would be much easier compare to the grinding the specimen alone.

Figure 3.5: Specimen that has been cold mount by using epoxy

Grinding process would take place using a grinding machine to smooth and flat up the specimen surface. To do that, a specified SiC paper that has different grit number would be utilized. Higher grit means that the SiC paper surface is smoother. For this specimen, the SiC paper been used are 180, 240, 400, 320 and 600.

Figure 3.6: Grinding machine and grinding process by using SiC paper

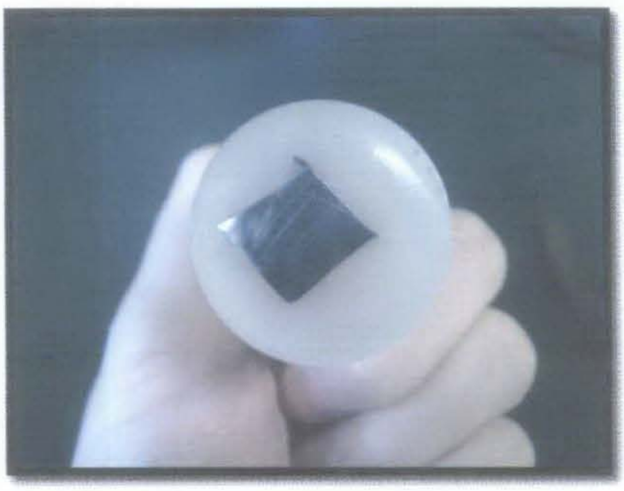

Figure 3.7: Specimen surface after grinding process

3.3 Experimental Setup

Experiments will be done by using a rotating cylinder electrode system and a potentiostat. The test assembly consists of one-liter glass cell bubbles with CO_2. The required test temperature is set through a hot plate. The electrochemical measurements are based on a three-electrode system. The reference electrode used is a saturated calomel electrode (SCE) and the auxiliary electrode is a platinum electrode

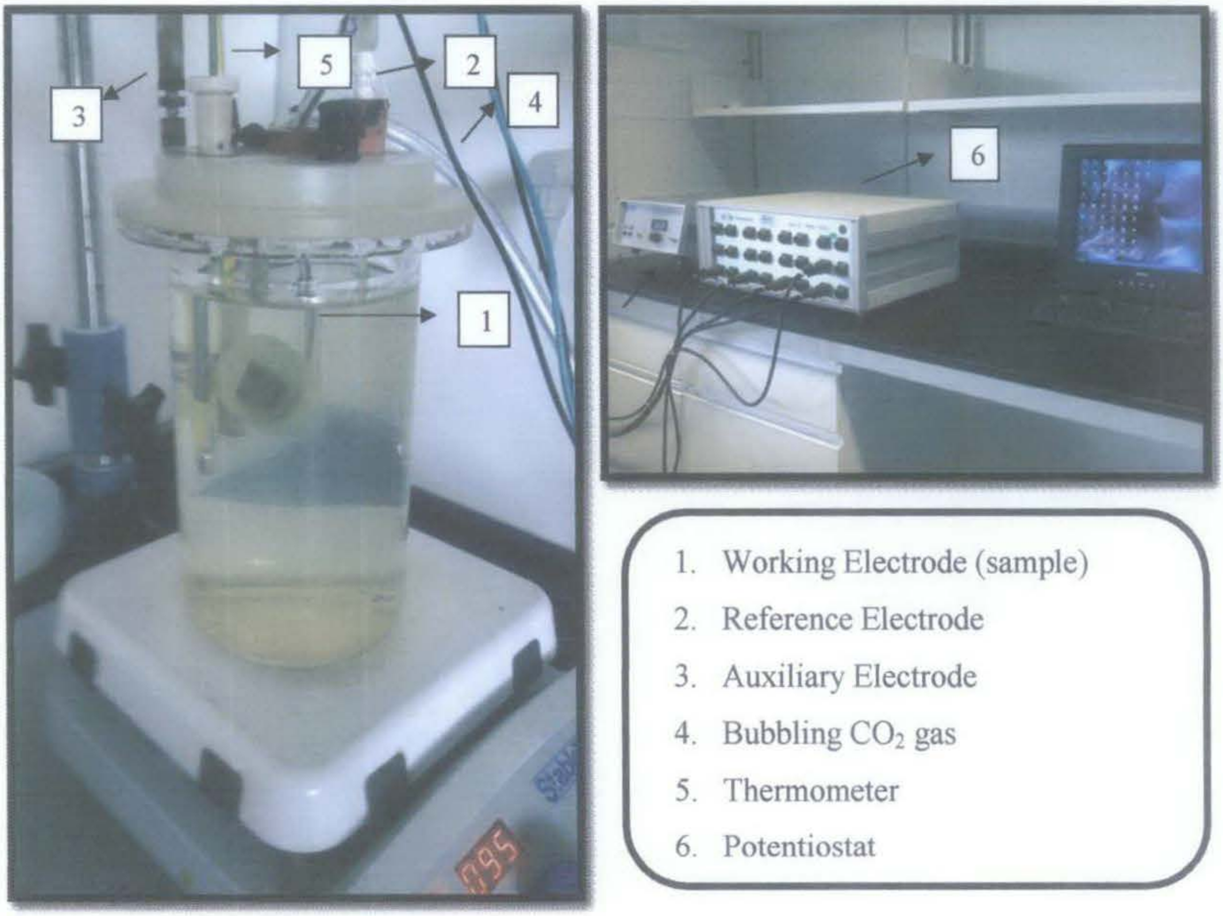

Figure 3.8: Experimental setup

Generally, the test matrix and procedure of the experiments is as shown at the table below:

Table 3.1: General test matrix

Parameter	Value
Steel Type	X52 carbon steel
Solution	3% NaCl
De-oxygenation gas	CO_2
pH	6.0
Temperature (°C)	50, 80
Fe^{2+} (ppm)	25, 50,100
Imidazoline (ppm)	25, 50
Rotational velocity (rpm)	0 or stagnant
Measurement techniques	LPR,EIS and SEM

General experimental procedure

1. Bubble CO_2 through 1-litre 3 % wt NaCl for an hour before put in the sample.
2. Adjust pH of the solution to the required values by adding solutions of 1M $NaHCO_3$, pH is measured at room temperature by pH meter.
3. Insert the mounted and grinded sample into glass cell and run the experiment.
4. Take the readings for analysis of LPR and EIS.
5. Repeat the procedure for the required temperatures and Fe^{2+} concentrations.

The test matrix is chosen to reflect the conditions in the field. In this project, there are two test studies that will be evaluated. Each of the studies differ in several parameters analyze and follow accordingly to the objectives.

Test Study 1: $FeCO_3$ Film Formation

Objectives:

- To study and analyze the formation of natural $FeCO_3$ film layer in CO_2 corrosion.
- To study the effect of multiple layers of $FeCO_3$ by inducing film formation.

Table 3.2: Test Matrix for test study 1

Parameter	Value
Steel Type	X52 carbon steel
Solution	3% NaCl
De-oxygenation gas	CO_2
pH	6.0
Temperature (°C)	50, 80
Fe^{2+} (ppm)	25
Rotational velocity (rpm)	0 or stagnant
Measurement techniques	LPR,EIS and SEM

Experimental procedure of Test study 1

1. Bubble CO_2 through 1-litre 3 % wt NaCl for an hour before put in the sample.
2. Adjust pH of the solution to pH 6.0 by adding solutions of 1M $NaHCO_3$. pH is measured at room temperature by pH meter. Set the temperature of the solution at 50 °C or 80 °C by using hot plate.
3. Insert the mounted and grinded sample into glass cell and run the experiment for period of 24 hours, representing natural $FeCO_3$ film formation as shown in Figure 3.9

1. **Carbon steel (CS) + $FeCO_3$ (single layer)**
   Conditions: pH = 6.0; T = 50°C and 80°C

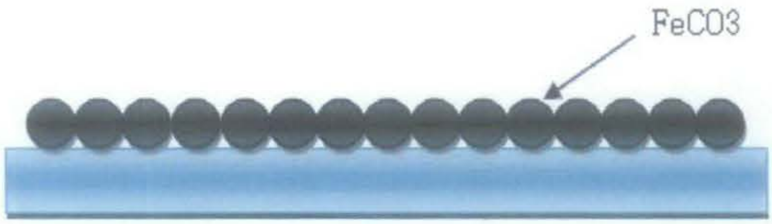

Figure 3.9: Schematic diagram for prediction of interaction between CS and single layer, fully protective $FeCO_3$

4. Inject 50ppm $FeCl_2$ to the solution after 8 hours of immersion, representing induced $FeCO_3$ film formation at 50°C and 80°C as shown in Figure 3.10 and Figure 3.11

2. **Carbon steel (CS) + $FeCO_3$ (multiple layer)**
   Conditions: pH = 6.0; T = 80°C; Induced Fe^{2+} iron = 25ppm

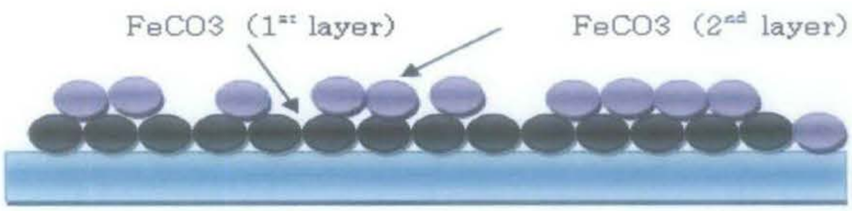

Figure 3.10: Schematic diagram for prediction of interaction between CS and multiple layers of $FeCO_3$ at 80°C

3. **Carbon steel (CS) + $FeCO_3$ (multiple layer)**
   Conditions: pH = 6.0; T = 50°C; Induced Fe^{2+} iron = 25ppm

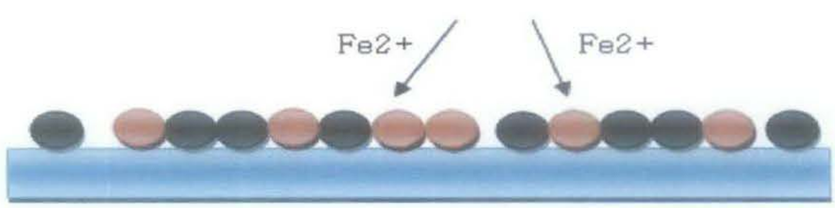

Figure 3.11: Schematic diagram for prediction of interaction between CS and multiple layers of $FeCO_3$ at 50°C

5. Take the readings for analysis of LPR and EIS at the end of experiment.

Hypothesis:

The aim of this test study is to analyze the formation of $FeCO_3$ film formation in case of fully protective protection, versus multiple layers of protective film layers. To see more understandable pattern and effectiveness of the protective layers, the figures above has been early predicted. Figure 3.10 and 3.11 are the prediction of $FeCO_3$ at temperature of 50 °C and 80 °C and would be a comparative measure for the other conditions.

The interaction between CS and multiple layer protective iron carbonate would indicate the effectiveness of this layer with regards to the corrosion rate value. The microstructure of multiple iron carbonate layer would have less porosity compare to single layer, thus would increase its strength. Less porous iron carbonate layer would leads to higher potential as diffusion barrier and resist corrosion on the metal surface.

To make more comparison, the study will then continue to predict the reaction of CS and iron carbonate layer at 50 °C and 80 °C together with induce Fe^{2+}. Besides that, the concentration of Fe^{2+} induce plays an important role as the right concentration would prove a significant difference in terms of the protection of $FeCO_3$ towards corrosion.

Test Study 2: $FeCO_3$ Film Formation and Corrosion Inhibitor

Objective:

- To study and analyze the interaction between formation of $FeCO_3$ film layer and corrosion inhibitor in CO_2 corrosion by different protective condition; under-saturation (50ppm Fe^{2+}) and saturation (100ppm Fe^{2+}).

Table 3.3: Test Matrix for test study 2

Parameter	Value
Steel Type	X52 carbon steel
Solution	3% NaCl
De-oxygenation gas	CO_2
pH	6.0
Temperature (°C)	50
Imidazoline (ppm)	25
Fe^{2+} (ppm)	50, 100
Rotational velocity (rpm)	0 or stagnant
Measurement techniques	LPR,EIS and SEM

Experimental procedure of Test study 2

1. Bubble CO_2 through 1-litre 3 % wt NaCl for an hour before put in the sample.
2. Adjust pH of the solution to pH 6.0 by adding solutions of 1M $NaHCO_3$. pH is measured at room temperature by pH meter. Set the temperature of the solution at 50 °C by using hot plate.
3. Insert the mounted and grinded sample into glass cell and run the experiment for period of 24 hours. Induced 50ppm $FeCl_2$ into the solution.
4. Inject 25ppm imidazoline to the solution after 4 hours of immersion.
5. Take the readings for analysis of LPR and EIS at the end of experiment.
6. Repeat the procedure for concentration of induced 100ppm Fe^{2+}.

Corrosion inhibitor deployment

1. **Carbon steel (CS) + Corrosion Inhibitor (CI)**

   Conditions: pH = 6.0; T = 50 °C; CI concentration = 50ppm

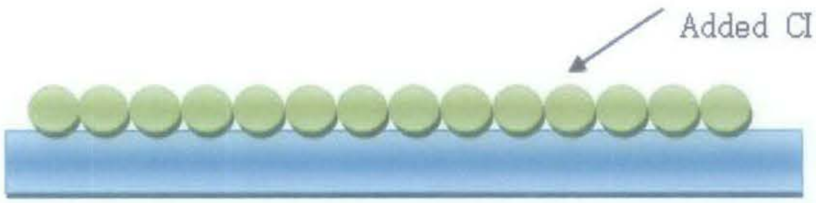

Figure 3.12: Schematic diagram for prediction of interaction between CS and fully protection from CI

2. **Carbon steel (CS) + Corrosion Inhibitor (CI)**

   Conditions: pH = 6.0; T = 50 °C; CI concentration = 25ppm

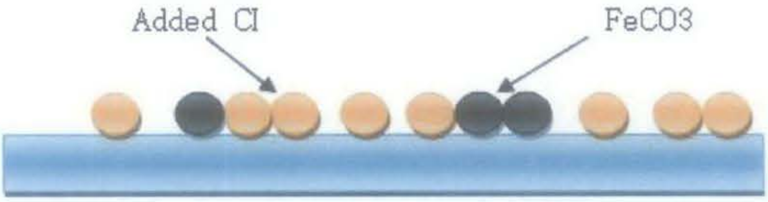

Figure 3.13: Schematic diagram for prediction of interaction between CS and semi-protection from CI

Corrosion inhibitor deployment and induced $FeCO_3$ film formation

1. **Carbon steel (CS) + Corrosion Inhibitor (CI) + $FeCO_3$ (induced Fe^{2+})**

   Conditions: pH = 6.0; T = 50 °C; CI concentration = 25ppm;

   Fe2+ concentration = 50 ppm & 100 ppm

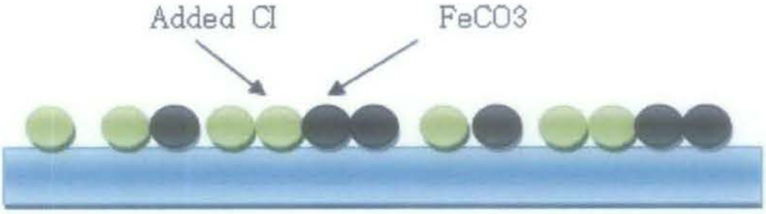

Figure 3.14: Schematic diagram for prediction of interaction between CS, semi-protection from CI and $FeCO_3$ by inducing Fe^{2+}

Hypothesis:

The aim of this test study is to analyze and to discover the potential corrosion protection by inducing film protection. As what been revised in the problem statement, the industry still rely on the deployment of corrosion inhibitors. To encounter the situation, the interaction CI together with $FeCO_3$ would be investigated to observe the effectiveness and how it will help in reducing the corrosion effects.

The investigation would begin with the interaction study between CS and using fully protection of CI. The expected concentration CI is 50ppm as it would increase the inhibitor efficiency to 98% in reducing the corrosion rate [5]. The time needed to fully protect the metal surface and have constant corrosion rate would be noted as point of reference for this particular study. An interaction between CS and semi-protection of CI would be evaluated to see how the CI would react with that much of concentration.

As a comparison, another test will be carried out by inducing Fe^{2+} to the solution. The interaction between CI and $FeCO_3$ by inducing Fe^{2+} would create an adsorbing film that decrease the corrosion rate then when either the species alone [2]. This experiment would vary in Fe^{2+} concentration which would be at 50ppm and 100ppm and maintaining the concentration of CI at 25ppm to observe the interaction pattern and the significant change on how it would reduce the corrosion effect to the metal surface.

3.4 Electrochemical Measurement Techniques

3.4.1 Electrochemical Impedance Spectroscopy (EIS)

EIS was measured by applying a small amplitude sinuisoidal excitation potential with range between 5 to 10mV in the frequency range of 0.0001Hz to 100,000Hz. The data plotted is Nyquist plot, usually in semi-circle shape. The frequency of the plot determines the solution resistance and the diameter of the semi-circle represents the polarization resistance that relate with the calculation of corrosion rate. The measured Nyquist plot will be fitted by using EIS Spectrum Analyzer.

3.4.2 Linear Polarization Resistance (LPR)

LPR tests will be conducted by measuring the corrosion potential of the exposed sample and subsequently sweeping from -10mV to +10mV with a sweep rate of 10mV/min. This technique is based Stern-Geary equation that established due to Ohm's Law, as below:

$$i_{corr} = \frac{B}{R_p} \quad \text{where,} \quad B = \frac{b_a b_c}{2.303\,(b_a + b_c)} \qquad (3.1)$$

b_a and b_c are Tafel slopes for anodic and cathodic curves respectively.

CHAPTER 4
RESULTS AND DISCUSSIONS

4.1 Results

4.1.1 Test Study 1: $FeCO_3$ Film Formation

4.1.1.1 Natural $FeCO_3$ film formation

The corrosion rate measured by Linear Polarization Resistance (LPR) under natural film formation at 50 °C and 80 °C for 24 hours is shown in Figure 4.1.

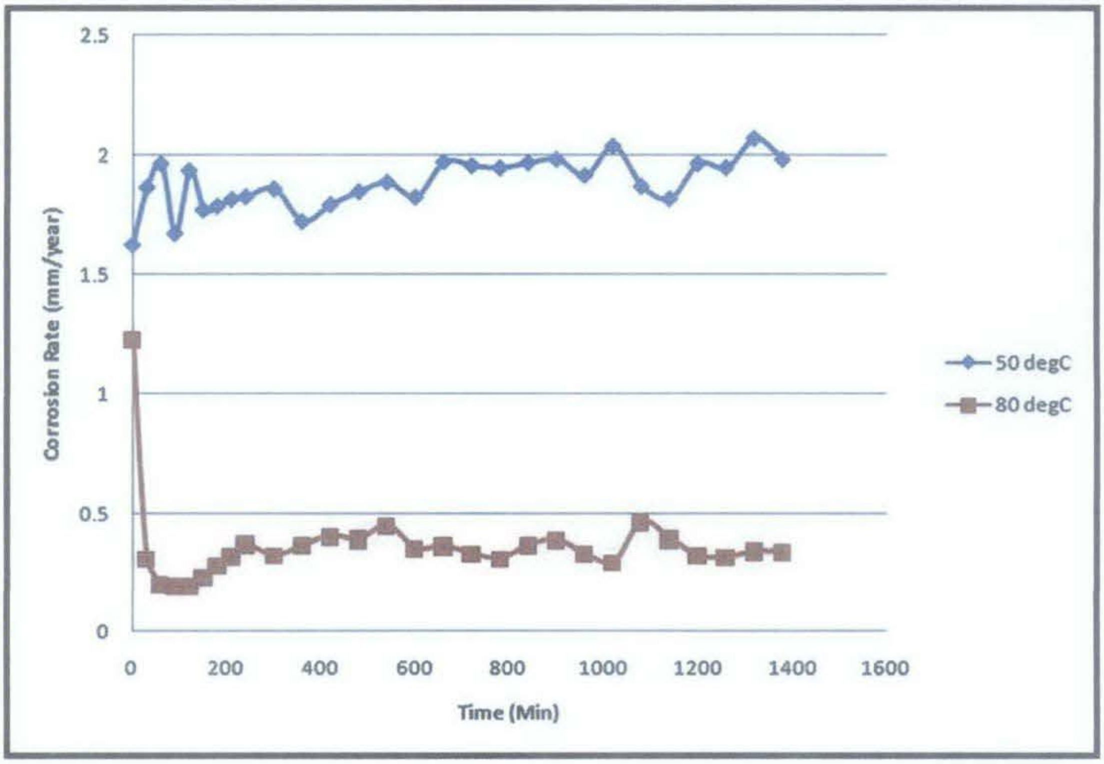

Figure 4.1: Corrosion rate recorded for 24 hours immersion of carbon steel specimen in CO_2 saturated 3 % wt NaCl solutions at temperature of 50 °C and 80 °C

The corrosion rate at 50 °C is higher than at 80 °C. The corrosion rate at 50 °C is at average of 1.8mm/year. However at 80 °C, the corrosion rate reduced from 1.2 mm/year to 0.3 mm/year. The reduction of corrosion rate at 80 °C indicating the formation of $FeCO_3$ film.

4.1.1.2 Induced $FeCO_3$ film formation

The corrosion rate measured by Linear Polarization Resistance (LPR) under induced film formation at 50 °C and 80 °C for 24 hours is shown in Figure 4.1.

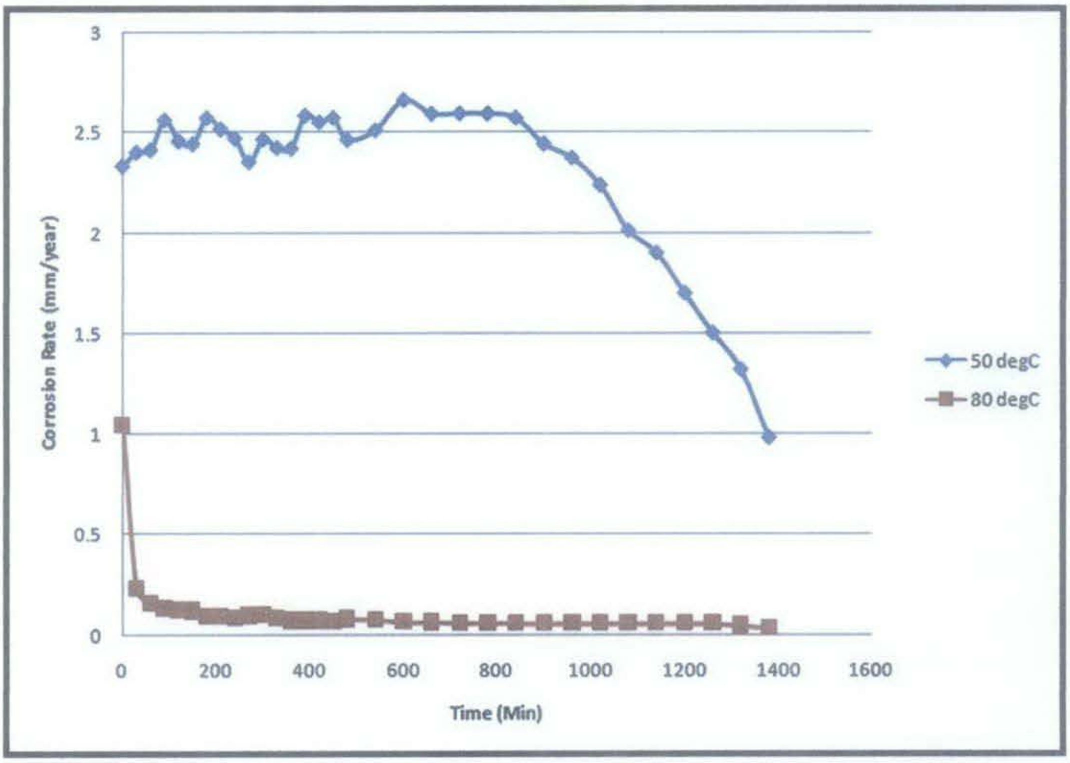

Figure 4.2: Corrosion rate recorded for 24 hours immersion of carbon steel specimen in CO_2 saturated 3 % wt NaCl solutions by inducing 25 ppm Fe^{2+} at temperature of 50 °C and 80 °C

From Figure 4.2, the initial recorded corrosion rate at 50 °C is 2.3 mm/year and reduced to 0.98 mm/year after 24 hours of immersion. At 80 °C, the initial corrosion rate is at 1.04 mm/year and stabilized at value of 0.04 mm/year. The reduction of the corrosion rate is due to the formation of $FeCO_3$ film.

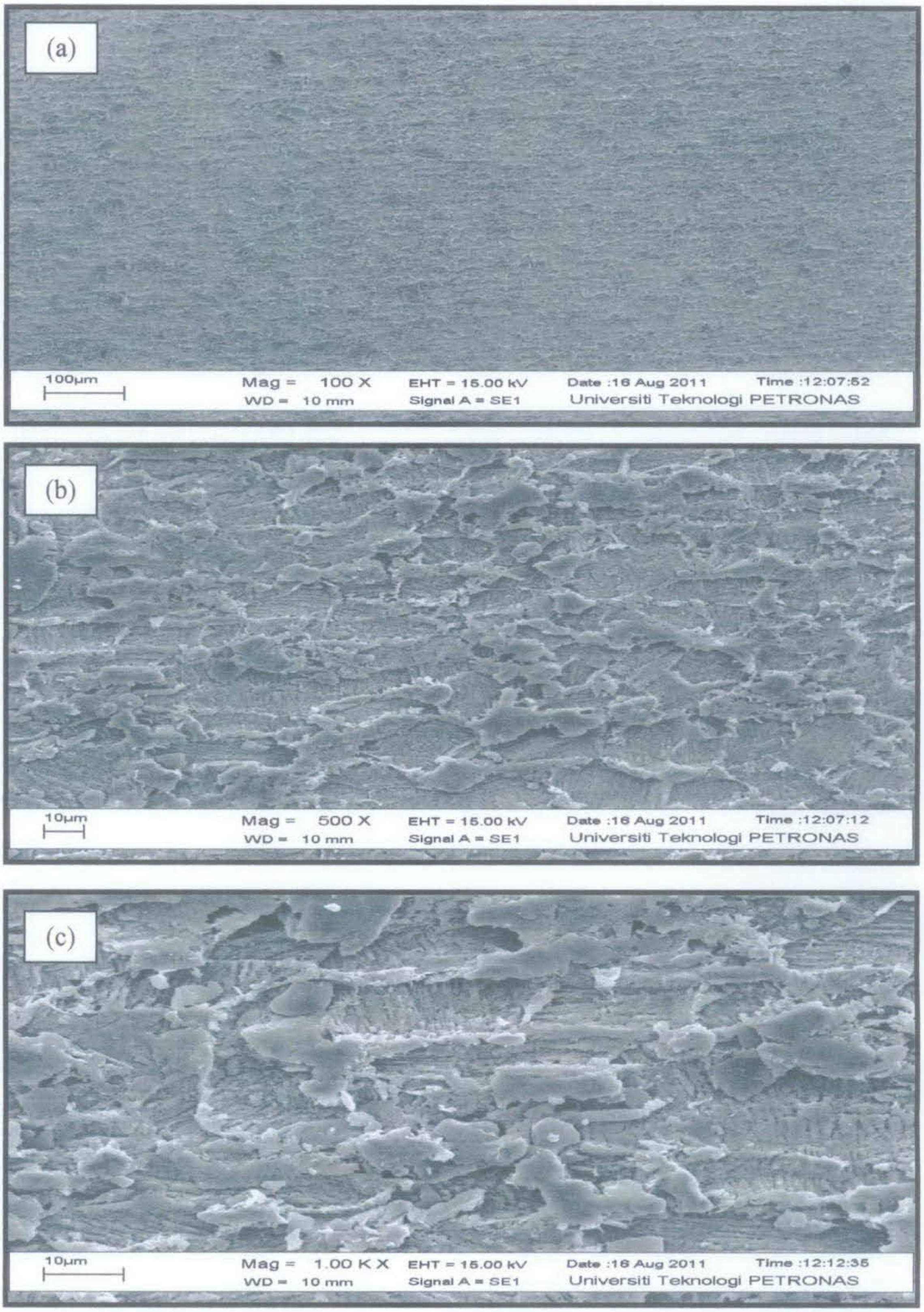

Figure 4.3: SEM images, for 24 hours of immersion for induced 25ppm Fe^{2+} at 50 °C

(a) 100X (b) 500X (c) 1000X

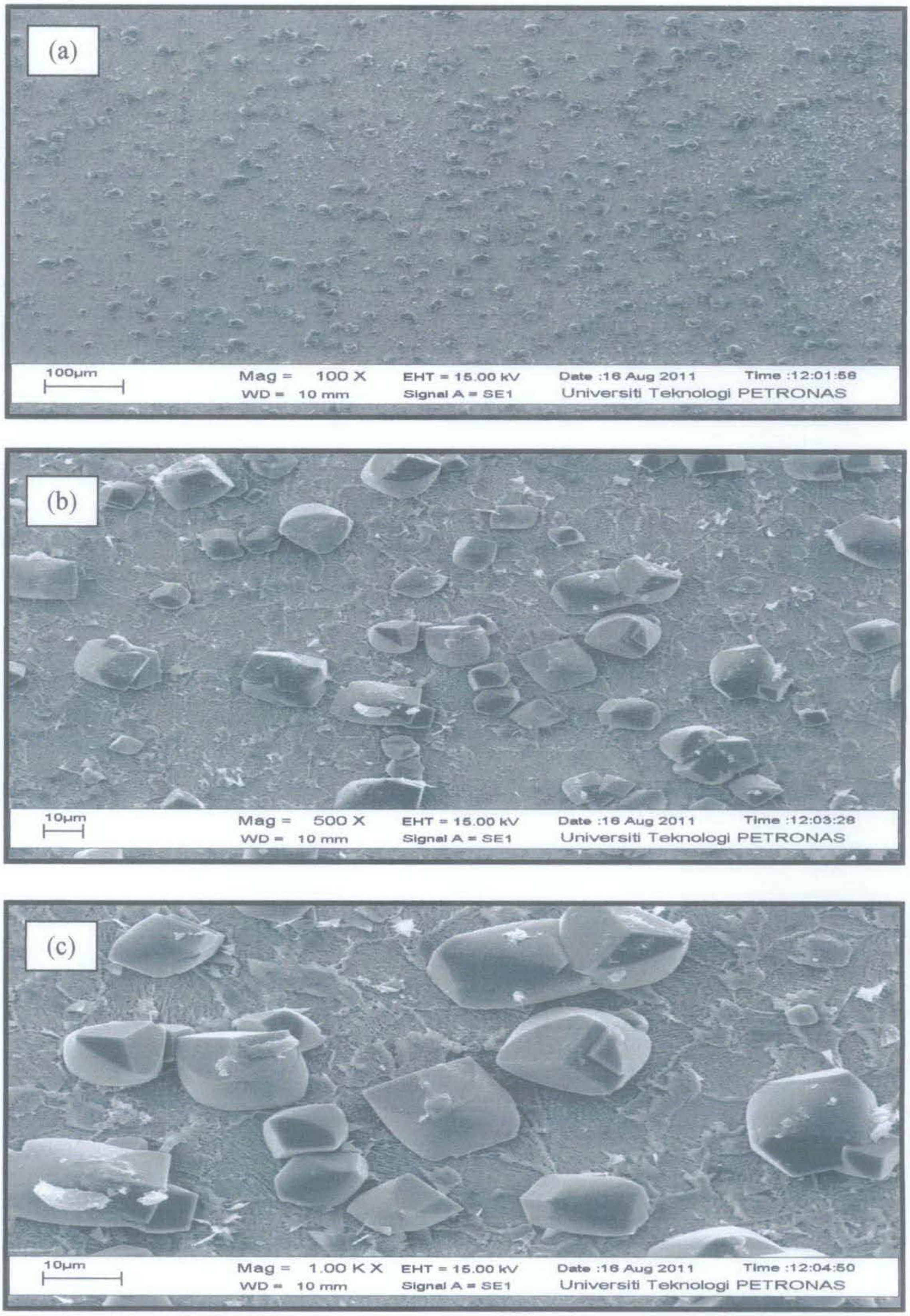

Figure 4.4: SEM images, for 24 hours of immersion for induced 25ppm Fe^{2+} at 80 °C

(a) 100X (b) 500X (c) 1000X

Scanning Electron Microscopy (SEM) images as in Figure 4.3 and Figure 4.4 show that the crystal grain formed at temperature 80 °C are apparent and thicker than at 50 °C. At 80 °C, the precipitation kinetics of $FeCO_3$ is higher compare to at 50 °C. Significantly, the product film can form faster and covered the surface to act as barrier for further corrosion attack. By inducing Fe^{2+}, the porosity of the film can be reduced as the solubility limit has been lowered. With that, the thickness of the layer can enhance the protection to the surface.

The reduction of corrosion rate observed under induced film formation proves the protective nature of film, particularly at 80 °C. The induced Fe^{2+} to the solution does help in reducing the rate of corrosion for both temperature as the increment in Fe^{2+} results in high supersaturation and helps in increasing the precipitation rate to form iron carbonate layer to fully protect the metal from further corrosion attack. The effect of the film can be observed from EIS spectrum.

Electrochemical Impedance Spectroscopy (EIS)

i. Natural $FeCO_3$ film formation

The Nyquist plot by Electrochemical Impedance Spectroscopy (EIS) under natural film formation at 50 °C and 80 °C for 24 hours is shown in Figure 4.5.

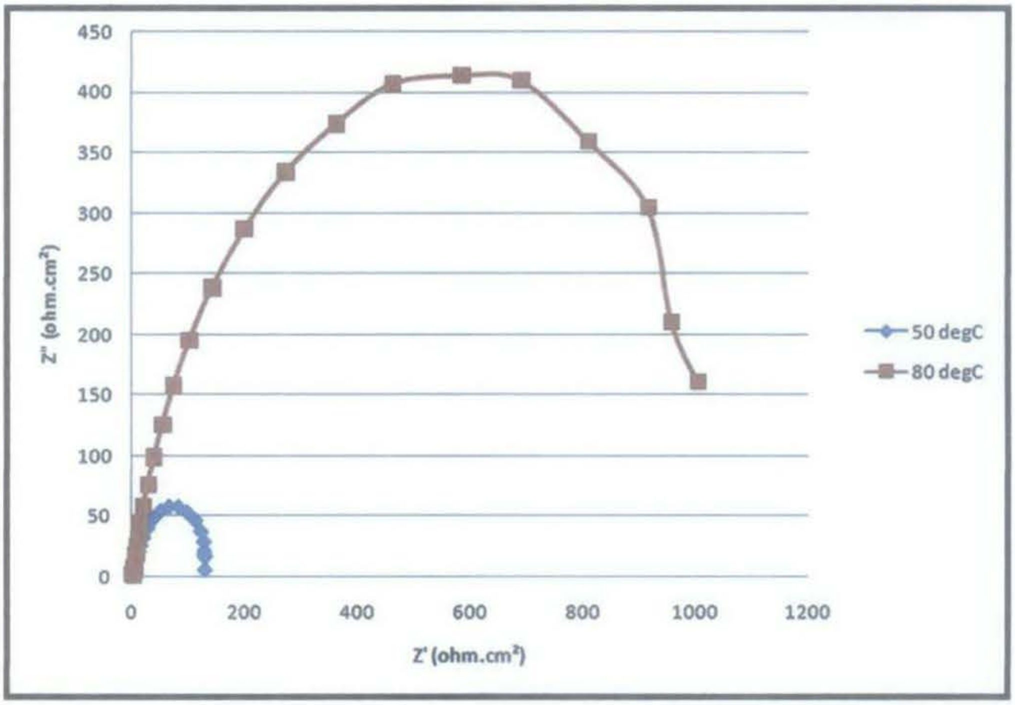

Figure 4.5: Nyquist plot recorded for 24 hours immersion of carbon steel specimen in CO_2 saturated 3 % wt NaCl solutions at temperature of 50 °C and 80 °C

From Figure 4.5, the diameter of semicircle for temperature of 80 °C is larger than at 50 °C. The diameter represents the resistance of the corrosion given by FeCO3 film. This shows that the polarization resistance is increasing and lead to lower corrosion effect. Significantly, the increment of temperature does help to reduce the corrosion rate and prove the growth of $FeCO_3$ layer [1].

ii. Induced $FeCO_3$ film formation

The Nyquist plot by Electrochemical Impedance Spectroscopy (EIS) under induced film formation at 50 °C and 80 °C for 24 hours is shown in Figure 4.6.

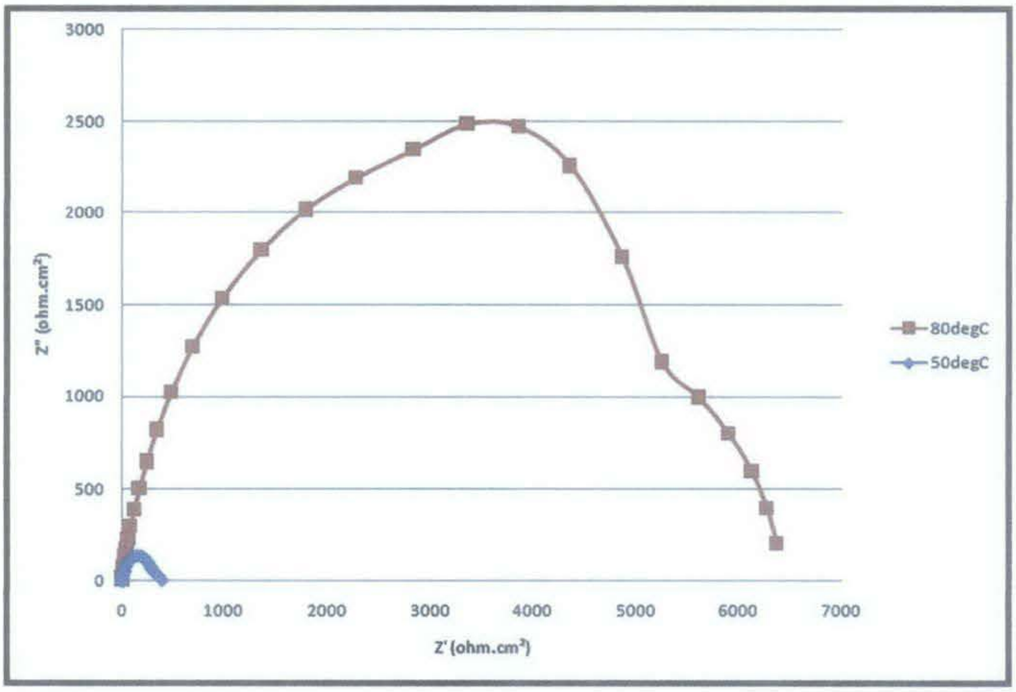

Figure 4.6: Nyquist plot recorded for 24 hours immersion of carbon steel specimen in CO_2 saturated 3 % wt NaCl solutions by inducing 25ppm Fe^{2+} at 50 °C and 80 °C

The corrosion rate and the formation of Nyquist plot at 80 °C outline a greater diameter of semicircle plot compare to the result at 50 °C. A higher potential resistance has been achieved and consequently the corrosion rate is reduced accordingly.

The formation of two semicircle plot from both temperatures indicates that there is formation of multiple layer of $FeCO_3$. The second semicircle form justify that there is diffusion process occur where the induced Fe^{2+} adsorb in the present film layer. It increases the film layer thickness and increase the protectiveness of the iron carbonate film to act as barrier and reduce the corrosion rate. At 80 °C, the second semicircle is more apparent than at 50 °C thus show that the precipitation rate will increase accordingly with increasing temperature.

Electrochemical Impedance Spectroscopy (EIS) Analysis

The graphs have been analyzed by using the EIS Analyzer (EISSA). The analyzer will interpret the data obtained from the ACM Sequencer by applying the equivalent circuit model. The model is chosen accordingly to the data obtained and resulting in minimal errors possible. The equivalent circuit model, fitted graphs and values obtained from the EISSA are as shown below.

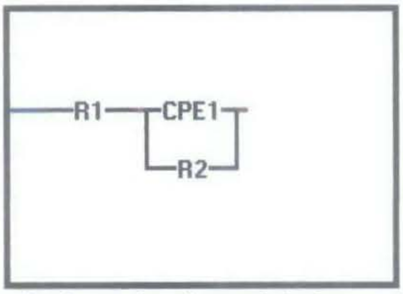

Figure 4.7: The equivalent circuit model chosen in EISSA software

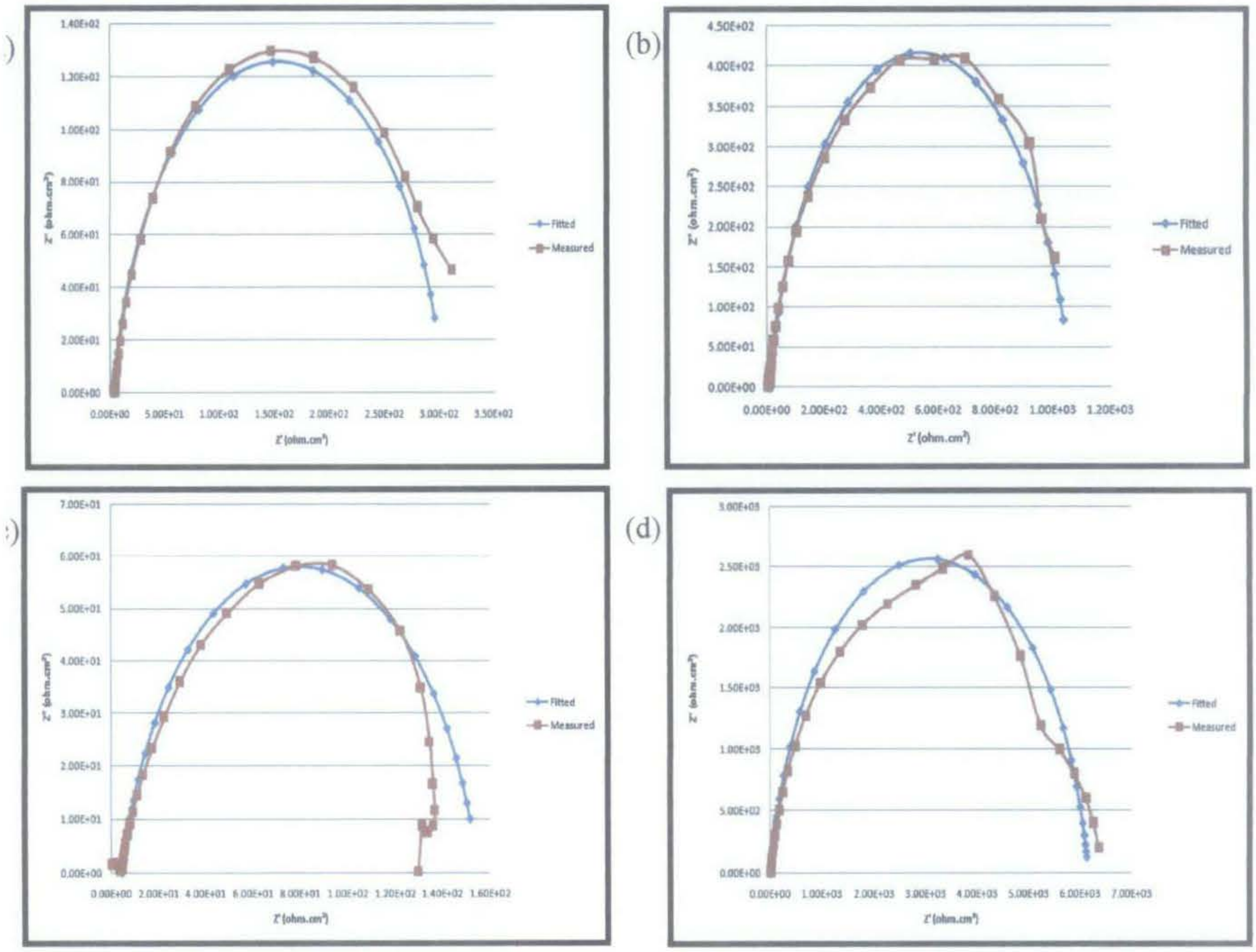

Figure 4.8: Nyquist plot comparison of experimental data and fitted results (a) 50 °C without induced Fe^{2+}, (b) 80 °C without induced Fe^{2+}, (c) 50 °C with induced Fe^{2+}, (d) 80 °C with induced Fe^{2+}

Table 4.1: Values of polarisation resistance, R_p (R2) obtained from EISSA

Conditions	**R_p (ohm.cm^2)**
50°C without induced Fe^{2+}	150.4
80 °C without induced Fe^{2+}	1050.7
50 °C with induced Fe^{2+}	300.9
80 °C with induced Fe^{2+}	6150.8

Polarization resistance, R_p values obtained from EISSA will be applied to calculate the corrosion current density, i_{corr} and finally the corrosion rate. R_p was given by Stern-Geary equation:

$$R_p = \frac{\Delta E}{\Delta I} = \frac{B}{i_{corr}} \quad \text{where, } B = \frac{b_a b_c}{2.303\,(b_c + b_c)} \tag{4.1}$$

b_a and b_c are Tafel slopes for anodic and cathodic curves respectively. The Stern-Geary constant, B is normally taken as 25mV as both anodic and cathodic reaction is activation controlled. The i_{corr} calculation is directly related from Faraday's Law:

$$CR\,(mm/year) = \frac{315 Z i_{corr}}{\rho n F} \tag{4.2}$$

where, CR = corrosion rate in mm/year

Z = atomic weight iron, 55.847 g/mole

i_{corr} = corrosion current density, μA/cm^2

p = density of iron, 7.8 g/cm^3

n = number of exchanged electrons

F = Faraday's constant, 96500 C/mole

Table 4.2: Values of i_{corr} and CR calculated

Conditions	EIS Analysis			LPR
	R_p (ohm.cm^2)	**i_{corr} ($\mu A/cm^2$)**	**CR (mm/year)**	**CR (mm/year)**
50°C without induced Fe^{2+}	150.4	166.22	1.94	1.62
80°C without induced Fe^{2+}	1050.7	23.79	0.28	0.34
50°C with induced Fe^{2+}	300.9	83	0.97	0.98
80°C with induced Fe^{2+}	6150.8	4.065	0.05	0.04

From Table 4.2, it is observed that the corrosion rate with induced Fe^{2+} is lower at both temperatures compare with without induced Fe^{2+}. The results have been compared to the LPR value, and it is seen that the measured data and fitted result matched well.

The corrosion rate trends at both 50°C and 80°C can be explained in terms of capacitance double layer (Cdl) values that can be obtained from EISSA analyzer. Cdl can be modelled by constant phase element, CPE as the capacitors in EIS often do not behave ideally [13]. CPE will counter the non-ideal behaviour of the layer by represent the surface roughness and non-uniformity of the surface resulted from the formation of deposit.

Table 4.3: Values of polarization resistance, R_p (R2) and capacitance double layer, (CPE) obtained from EISSA

Conditions	R_p (ohm.cm^2)	CPE (F)
50°C without induced Fe^{2+}	150.4	7.00E-04
80°C without induced Fe^{2+}	1050.7	2.14E-04
50°C with induced Fe^{2+}	300.9	5.05E-04
80°C with induced Fe^{2+}	6150.8	4.00E-05

From Table 4.3, it is observed that the CPE values are lower for both temperatures after inducing Fe^{2+} to the solution. Consequently, the decrement of the values could be related to the formation of $FeCO_3$ that resulting in more dense film layer on the metal surface. The growing of protective film layer has reduced the lack of homogeneity and the roughness of the film, thus reduce the CPE value.

Without inducing Fe^{2+} to the solution, the precipitation rate of iron carbonate layer is higher at temperature 80° C followed by at 50° C. Higher temperature will accelerate the precipitation kinetics of the film formation [14]. This indicates that at 50°C, kinetics of film formation is very much slower and limits the crystallization of $FeCO_3$ on the metal surface.

The same trend can be observed as induced Fe^{2+} has been done at the same temperature conditions. The formation of $FeCO_3$ is higher at 80°C and lowers at 50° C. Increasing the concentration of Fe^{2+} by inducing Fe^{2+} from external source into the solution has increased the supersaturation, therefore promotes the $FeCO_3$ film grow and increase the film density and thickness [14].

Induced Fe^{2+} at 50°C and 80°C has increase the film build up and fill the porous spaces to form dense and protective film [14]. As a result, the layer porosity is decrease and increases the thickness and density. To relate it with the CPE values obtained, the following relationship can be referred:

$$C_f = \frac{\varepsilon_f \varepsilon_0 A}{d} \tag{4.3}$$

where, d is the thickness of the layer, ε_f is the dielectric constant of the film, ε_0 is the dielectric constant of the material and A is the electrode surface. The capacitance (CPE) is inversely proportional to the density, hence has proven the decrement of CPE value as the density of the film increase and will result in lower corrosion rate.

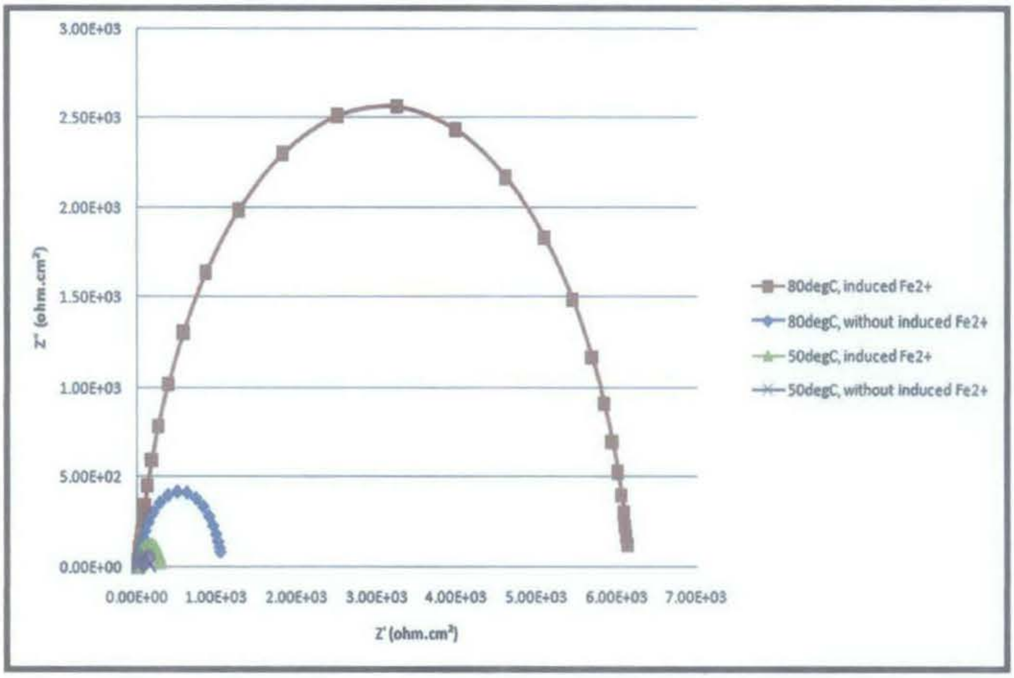

Figure 4.9: Comparison fitted Nyquist plot for test study 1

As a comparison, the fitted Nyquist plot from all 4 experiments has been plotted. The result does show that by inducing Fe^{2+}, the corrosion rate at 50 °C and 80 °C will decrease. However, a significant corrosion rate reduction can be observed at temperature 80 °C than 50 °C, either with or without inducing Fe^{2+}. From the study, temperature does play an important role in accelerating the precipitation kinetics of $FeCO_3$ film layer and lessen the corrosion effect.

4.1.2 Test Study 2: $FeCO_3$ Film Formation and Corrosion Inhibitor

4.1.2.1 Corrosion inhibitor deployment

The corrosion rate measured by Linear Polarization Resistance (LPR) by corrosion inhibitor deployment of imidazoline at 25ppm and 50ppm at 50°C for 24 hours is shown in Figure 4.10.

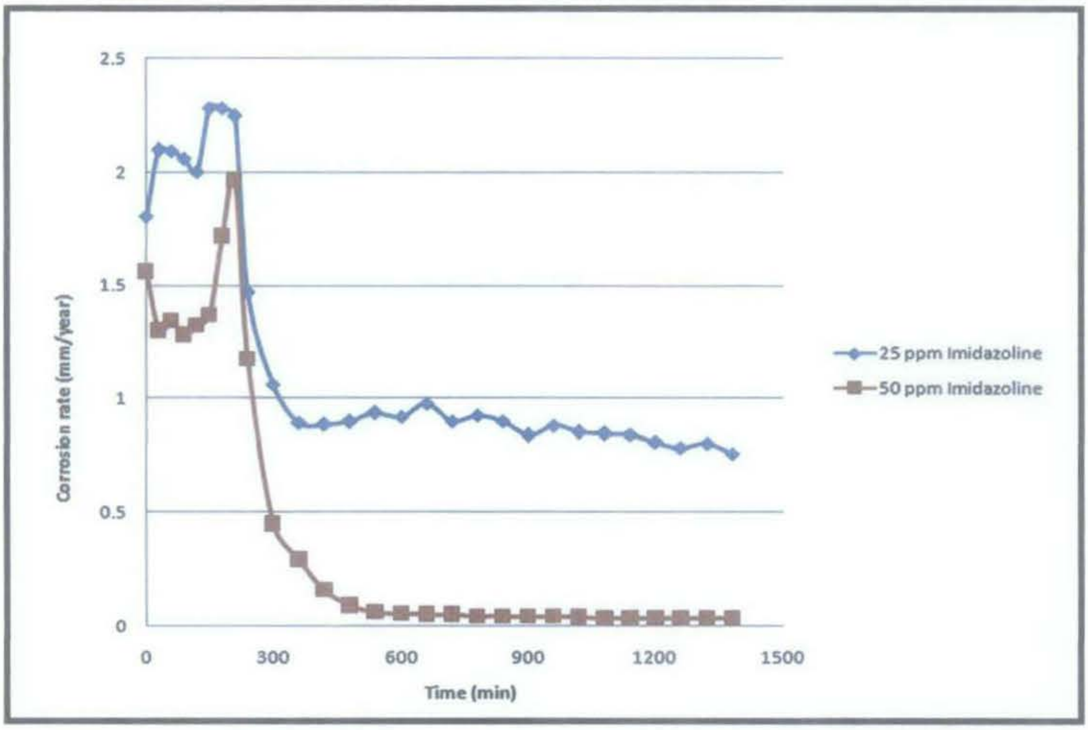

Figure 4.10: Corrosion rate recorded for 24 hours immersion of carbon steel specimen in CO_2 saturated 3 % wt NaCl solutions at temperature of 50°C and induced 25ppm Fe^{2+} in addition with 25ppm and 50ppm imidazoline respectively

The corrosion rates for both studies are reducing with respect to time. To see the comparison, imidazoline inhibitor has been injected to the solution after 4 hours of immersion. The results showed that the corrosion rates drop rapidly from initially 2.28 mm/year to 1.47mm/year for addition of 25ppm of imidazoline and from 1.56 mm/year to 0.45mm/year for addition of 50ppm of imidazoline. The final corrosion rates for addition of 25ppm and 50ppm imidazoline are 0.76 mm/year and 0.03 mm/year respectively.

4.1.2.2 Corrosion inhibitor deployment and induced $FeCO_3$ film formation

The corrosion rate measured by Linear Polarization Resistance (LPR) by corrosion inhibitor deployment of imidazoline at 25ppm together with 50ppm and 100ppm of induced Fe^{2+} at 50 °C for 24 hours is shown in Figure 4.11.

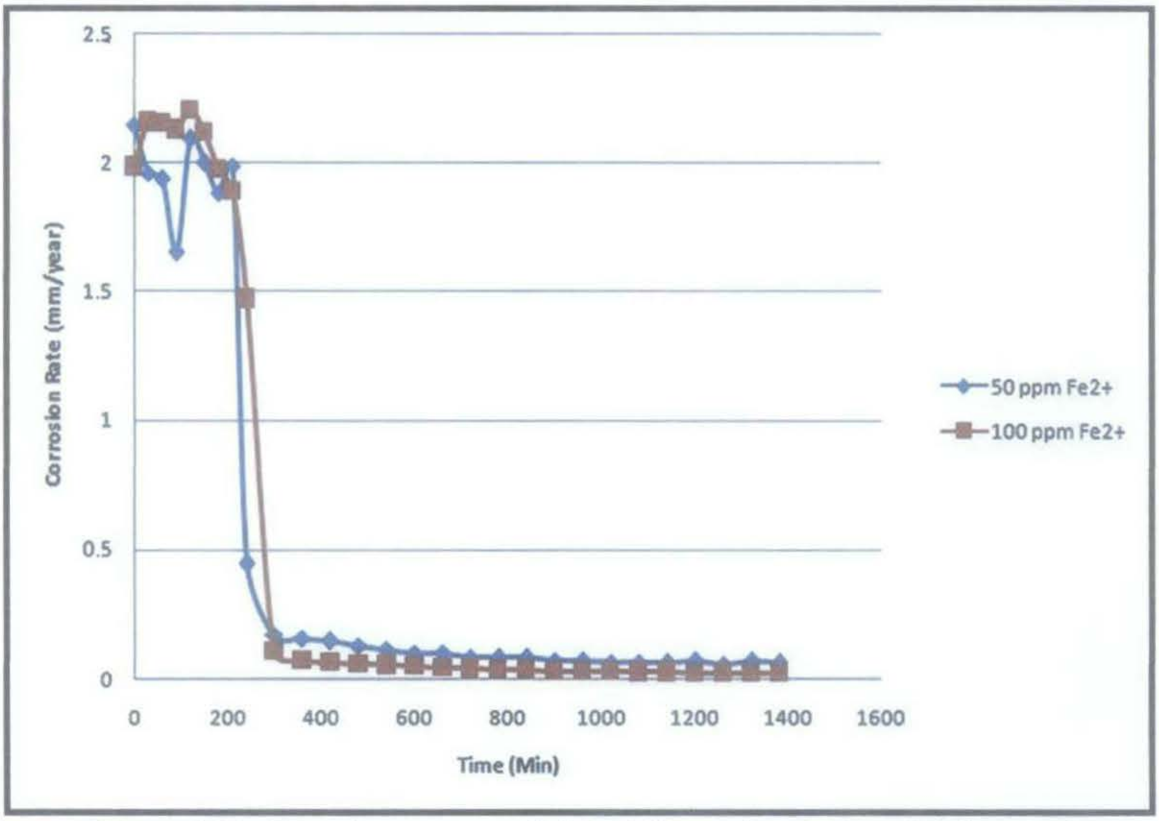

Figure 4.11: Corrosion rate recorded for 24 hours immersion of carbon steel specimen in CO_2 saturated 3 % wt NaCl solutions at temperature of 50 °C and induced 25ppm imidazoline in addition with 50ppm and 100ppm Fe^{2+} respectively

From the graph plotted shown in Figure 4.11, the corrosion rate for 100ppm induced Fe^{2+} is much lower compare to the 50ppm induced Fe^{2+}. The initial recorded corrosion rate for induced 50ppm Fe^{2+} is 2.15 mm/year and reduced to 0.06 mm/year after 24 hours of immersion. At 100ppm induced Fe^{2+}, the initial corrosion rate is at 2.15 mm/year and stabilized at value of 0.02 mm/year.

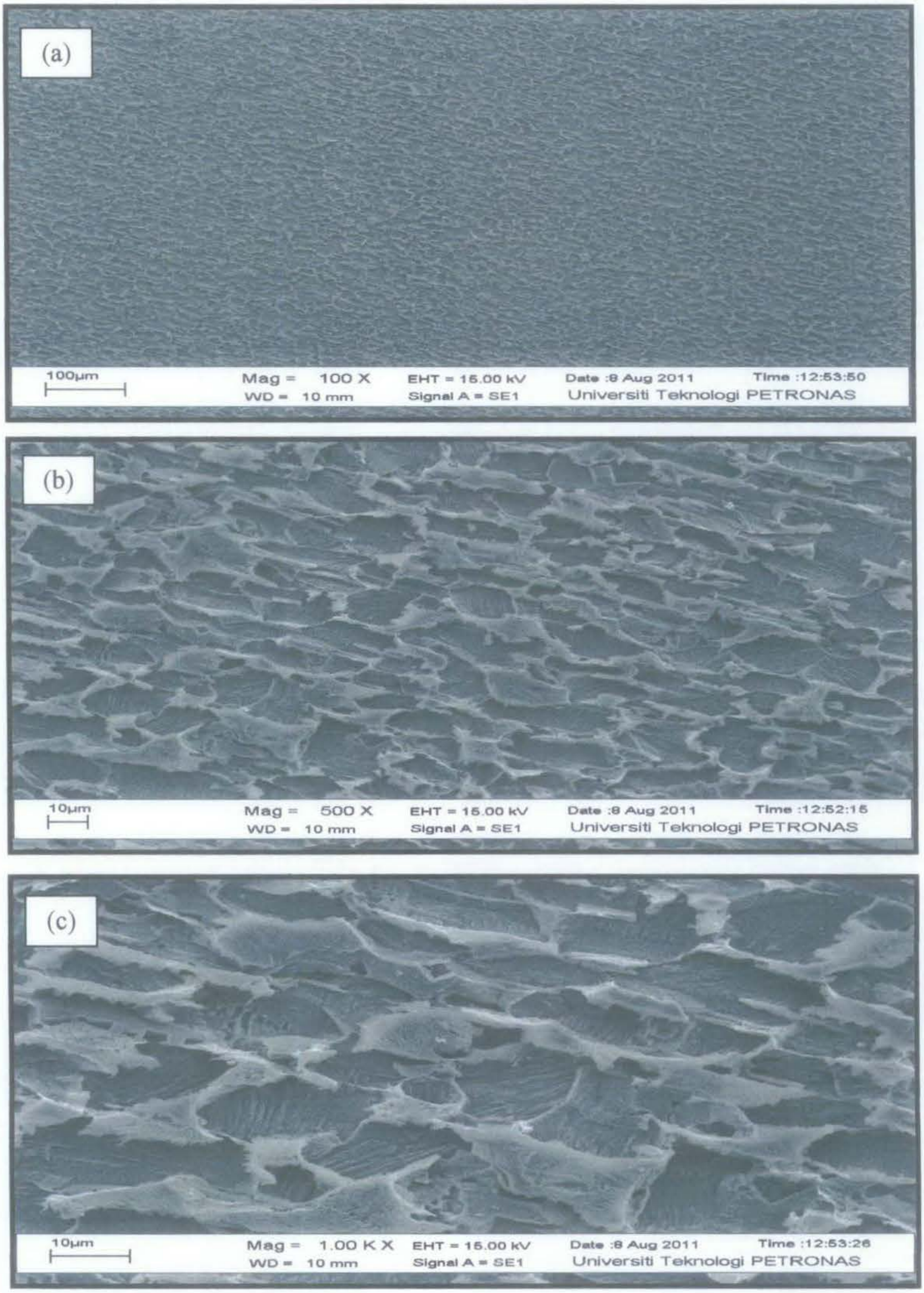

Figure 4.12: SEM images, for 24 hours of immersion of 25ppm of imidazoline and induced 100ppm Fe^{2+} (a) 100X (b) 500X (c) 1000X

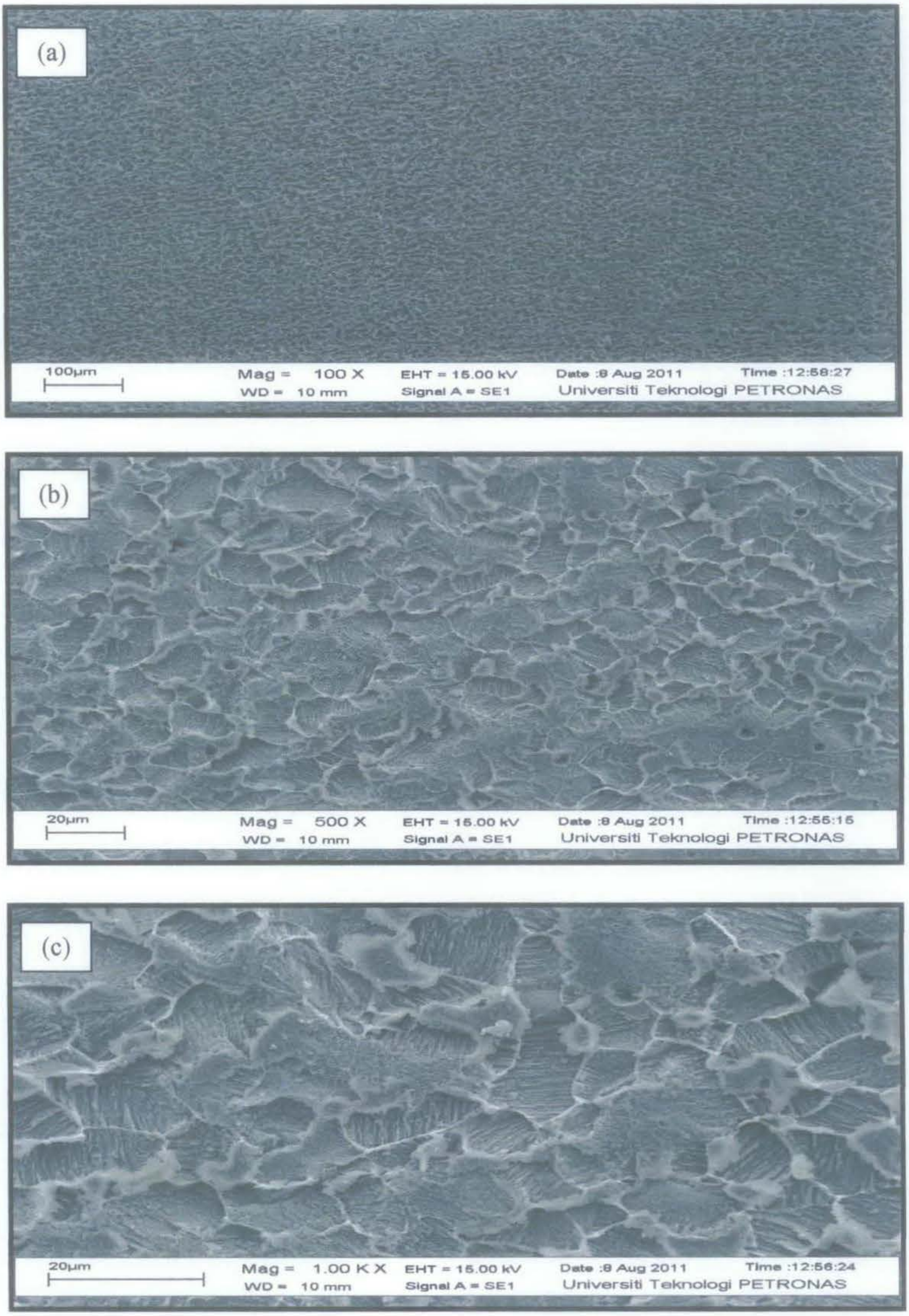

Figure 4.13: SEM images, for 24 hours of immersion of 25ppm of imidazoline and induced 50ppm Fe^{2+} (a) 100X (b) 500X (c) 1000X

Scanning Electron Microscopy (SEM) images from Figure 4.12 and Figure 4.13 shows that by inducing 100ppm Fe^{2+} together with 25ppm imidazoline, the precipitates formed are slightly bigger and more compact than inducing at 50ppm Fe^{2+} .This does show that there is interaction between $FeCO_3$ and imidazoline to form a protective layer. By increasing the concentration of induced Fe^{2+}, the thickness of the film form is increase and gives greater protection to the metal surface.

From the graph trend, the corrosion rate would reduce accordingly and induced $FeCO_3$ will interact with imidazoline inhibitor. Higher concentration of Fe^{2+} induced, the lower the corrosion rate would be. The induced Fe^{2+} would still aid in increasing the supersaturation thus increase the precipitation rate to form the iron carbonate film layer. Another finding that can be seen is the effect of imidazoline inhibitor itself to help in reducing the rate of corrosion. For both graphs, imidazoline inhibitor significantly drops the corrosion rate after it been injected after 4 hours of immersion. This indicates the inhibitor major role in reducing the effect of corrosion.

TASK	DURATION	START	END	1	2	3	4	5	6	7	8	9	10	11	12	13	14	15
1	1 day	Mon (26/5/11)	Mon (26/5/11)															
2	33 days	Wed (25/5/11)	Fri (8/7/11)															
3	7 days	Mon (4/7/11)	Sun (10/7/11)															
4	1 day	Fri (15/7/11)	Fri (15/7/11)								▽							
5	25 days	Mon (11/7/11)	Fri (12/8/11)															
6	7 days	Mon (25/8/11)	Sun (31/7/11)															
7	1 day	Fri (5/8/11)	Fri (5/8/11)										▽					
8	11 days	Mon (1/8/11)	Thu (11/8/11)															
9	1 day	Fri (12/8/11)	Fri (12/8/11)												▽			
10	11 days	Mon (8/8/11)	Thu (18/8/11)															
11	1 day	Fri (19/8/11)	Fri (19/8/11)													▽		
12	7 days	Mon (15/8/11)	Sun (21/8/11)															
13	1 day	TBA	TBA														▽	
14	7 days	Mon (22/8/11)	Sun (28/8/11)															
15	1 day	Fri (2/9/11)	Fri (2/9/11)															▽

1 : FYP 2 Briefing

2 : Project work continues

3 : Progress report preparation

4 : Submission of progress report

5 : Project work continues

6 : Pre-EDX preparation

7 : Pre-EDX

8 : Draft report preparation

9 : Submission of draft report

10 : Technical paper and dissertation (soft bound) preparation

11 : Submission of technical paper and dissertation (soft bound)

12 : Oral presentation preparation

13 : Oral presentation

14 : Dissertation (hard bound) preparation

15 : Submission of dissertation (hardbound)

The test continues by inducing Fe^{2+} together with imidazoline inhibitor to the solution to analyze the interaction between $FeCO_3$ films with imidazoline inhibitor. Concentration of Fe^{2+} used varies of 50ppm and 100ppm and induced at the beginning of the test and imidazoline with concentration of 25ppm has been injected to the solution after 4 hours of immersion for both tests.

ii. Corrosion inhibitor deployment and induced $FeCO_3$ film formation

The Nyquist plot by Electrochemical Impedance Spectroscopy (EIS) under corrosion inhibitor deployment of imidazoline at 25ppm together with 50ppm and 100ppm induced Fe^{2+} at 50 °C for 24 hours is shown in Figure 4.11.

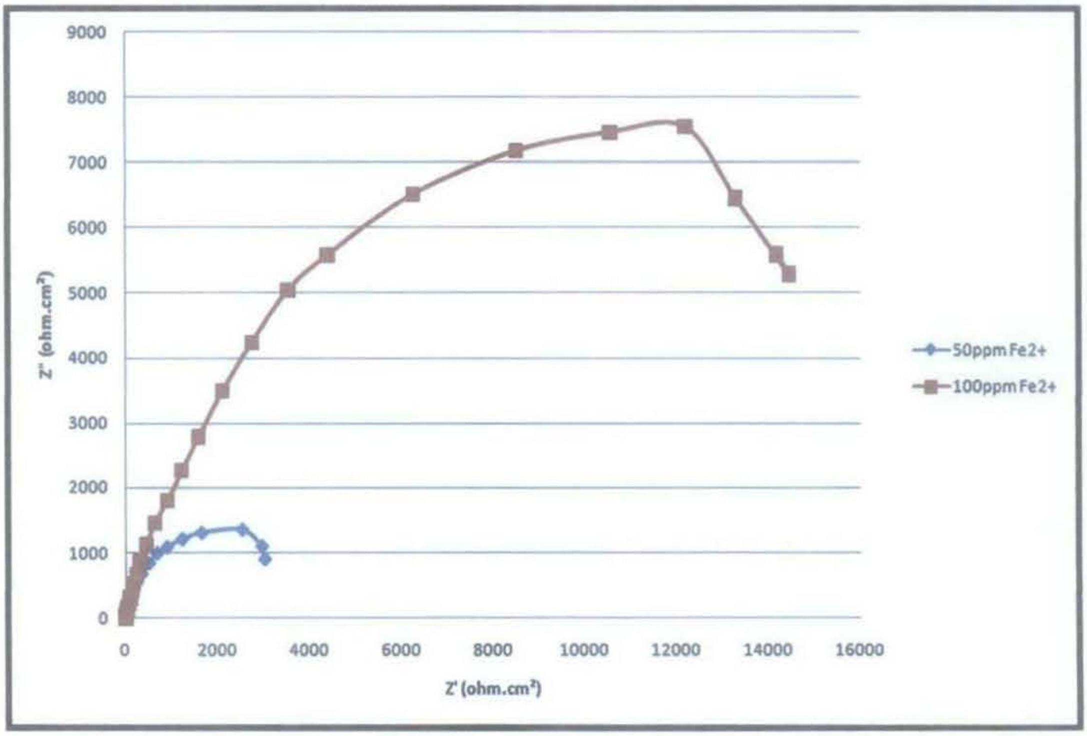

Figure 4.15: Nyquist plot recorded for 24 hours immersion of carbon steel specimen in CO_2 saturated 3 % wt NaCl solutions at temperature of 50 °C and induced 50ppm and 100ppm Fe^{2+} together with 25ppm imidazoline

The semicircle of the Nyquist plot for interaction between 100ppm Fe^{2+} and 25ppm imidazoline has bigger diameter compare to the plot for 50ppm Fe^{2+} and 25ppm imidazoline. This indicates that the effect of interaction between inhibitor with higher concentration of Fe^{2+} is possible and gives greater protection to the metal surface.

By inducing 100ppm Fe^{2+}, the precipitation rate of iron carbonate film formation is increasing as a very high saturation is needed to form the protective film and to obtain a successful protection. With the aid from imidazoline, the corrosion rate reduces significantly as shown at Figure 4.15. This is because the inhibitor act and remain as the major factor in reducing the rate of corrosion.

Electrochemical Impedance Spectroscopy (EIS) Analysis

Based on the results, the EIS Analyzer (EISSA) will again be utilized. The analyzer will interpret the data obtained from the ACM Sequencer by applying the equivalent circuit model. The model is chosen accordingly to the data obtained and resulting in minimal errors possible. The equivalent circuit model, fitted graphs and values obtained from the EISSA are as shown below:

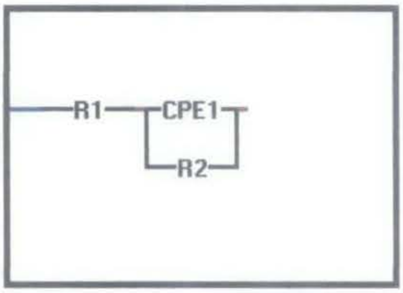

Figure 4.16: The equivalent circuit model chosen in EISSA software

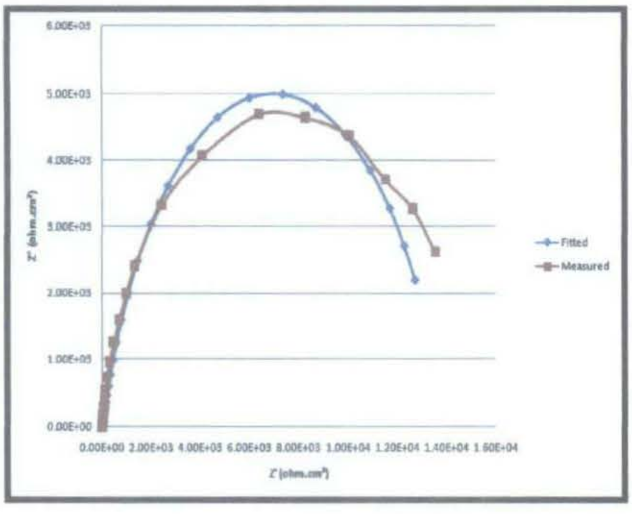

(b)

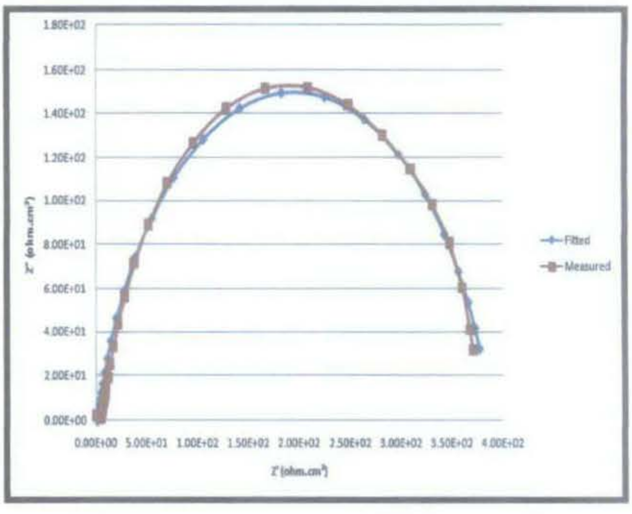

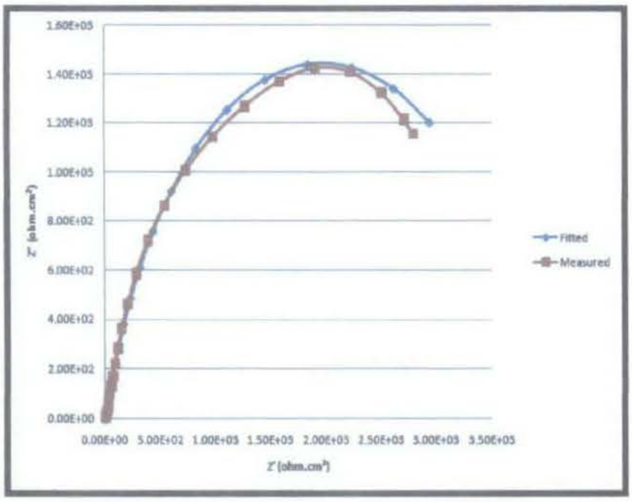

(d)

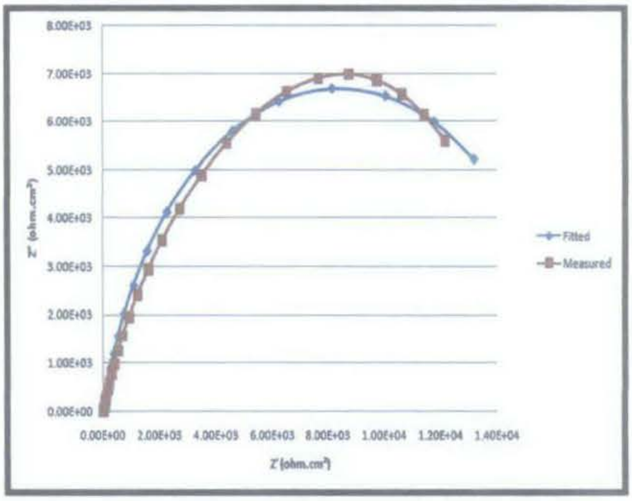

Figure 4.17: Nyquist plot comparison of experimental data and fitted results (a) 50ppm imidazoline, (b) 25ppm imidazoline, (c) 50ppm Fe^{2+} and 25ppm imidazoline, (d) 100ppm Fe^{2+} and 25ppm imidazoline

Table 4.4: Values of polarization resistance, R_p (R2) obtained from EISSA

Conditions	R_p (ohm.cm^2)
50ppm imidazoline	13905
25ppm imidazoline	387.99
50ppm Fe^{2+} and 25ppm imidazoline	3937.8
100ppm Fe^{2+} and 25ppm imidazoline	16876

Polarization resistance, R_p values obtained from EISSA will be applied to calculate the corrosion current density, i_{corr} and finally the corrosion rate. R_p was given by Stern-Geary equation:

$$R_p = \frac{\Delta E}{\Delta I} = \frac{B}{i_{corr}} \quad \text{where,} \quad B = \frac{b_a b_c}{2.303\,(b_a + b_c)} \tag{4.4}$$

b_a and b_c are Tafel slopes for anodic and cathodic curves respectively. The Stern-Geary constant, B is normally taken as 25mV as both anodic and cathodic reaction is activation controlled. The i_{corr} calculation is directly related from Faraday's Law:

$$CR\ (mm/year) = \frac{315 Z i_{corr}}{\rho n F} \tag{4.5}$$

where, CR = corrosion rate in mm/year

Z = atomic weight iron, 55.847 g/mole

i_{corr} = corrosion current density, µA/cm^2

p = density of iron, 7.8 g/cm^3

n = number of exchanged electrons

F = Faraday's constant, 96500 C/mole

Table 4.5: Values of i_{corr} and CR calculated

	EIS Analysis			LPR
Conditions	**R_p (ohm.cm^2)**	**i_{corr} (µA/cm^2)**	**CR (mm/year)**	**CR (mm/year)**
50ppm imidazoline	13905	1.798	0.02	0.03
25ppm imidazoline	387.99	64.43	0.75	0.76
50ppm Fe^{2+} and 25ppm imidazoline	3937.8	6.349	0.07	0.06
100ppm Fe^{2+} and 25ppm imidazoline	16876	1.48	0.02	0.02

From Table 4.5, it is observed that the corrosion rate by injecting high concentration of imidazoline is reduced. Consequently, the rate of corrosion by interaction between imidazoline and induced Fe^{2+} is slightly lower compare to the usage of 25ppm and 500ppm imidazoline. With the result obtained, it is proven that by inducing Fe^{2+} to increase the formation of $FeCO_3$ will create an adsorbing film that decrease the corrosion rate and increase the film impedance more so than when either species is alone [2]. The results have been compared to the LPR value, and it is seen that the measured data and fitted result matched well.

The corrosion rate trends for the tests can be explained in terms of capacitance double layer (Cdl) values that can be obtained from EISSA analyzer. Cdl can be modelled by constant phase element, CPE as the capacitors in EIS often do not behave ideally [13]. CPE will counter the non-ideal behaviour of the layer by represent the surface roughness and non-uniformity of the surface resulted from the formation of deposit.

Table 4.6: Values of polarization resistance, R_p (R2) and capacitance double layer, (CPE) obtained from EISSA

Conditions	R_p (ohm.cm^2)	CPE (F)
50ppm imidazoline	13905	2.82E-04
25ppm imidazoline	387.99	4.57E-04
50ppm Fe^{2+} and 25ppm imidazoline	3937.8	4.03E-04
100ppm Fe^{2+} and 25ppm imidazoline	16876	1.25E-04

From Table 4.6, it is observed that the CPE values are lower for the test by combination of imidazoline and induced Fe^{2+} if compare by the tests by using only imidazoline. The result is corresponding to the R_p values obtained where increasing R_p would result in decreasing CPE value.

By applying imidazoline at 25ppm and 50ppm, the inhibitor film layer form on the surface of the metal. Increasing the concentration of imidazoline inhibitor into the solution will increase the thickness and the density of the inhibitor film [12]. The adsorbed imidazoline molecules have blocked the active sites on the metal surface thus resulting in lower corrosion rate and give greater protection [11].

For the case of combination of imidazoline and induced Fe^{2+}, the formation of $FeCO_3$ by inducing100ppm of Fe^{2+} ions has increased the supersaturation of $FeCO_3$ to form on the metal surface. Therefore, the film form is denser and slightly thicker if compare with induced 50ppm Fe^{2+}. However, the precipitation of $FeCO_3$ is described as slow and temperature dependent [9]. At 50 °C, the precipitation of $FeCO_3$ film is porous and not fully protective to the metal surface.

Induced 25ppm imidazoline for both tests have given a major impact as the corrosion rate is reduced significantly. Theoretically, imidazoline molecules presumably been adsorbed on an inner film of $FeCO_3$ and takes place very quickly [12]. The increase in the compactness of the layer has closed the porosity and thus increasing the density. This can be proven by following relationship:

$$C_f = \frac{\varepsilon_f \varepsilon_0 A}{d} \qquad (4.6)$$

where, d is the thickness of the layer, ε_f is the dielectric constant of the film, ε_0 is the dielectric constant of the material and A is the electrode surface. The capacitance (CPE) reduction results from Table 4.6 have proven that the thickness of the film is increase.

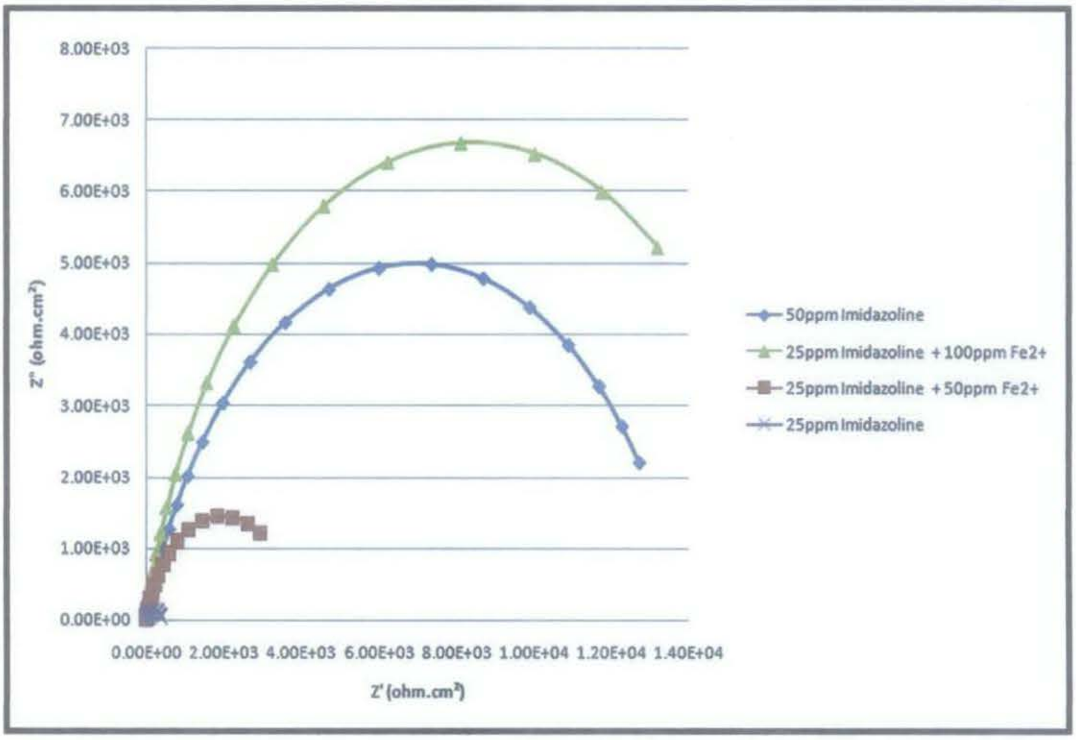

Figure 4.18: Comparison fitted Nyquist plot for test study 2

As a comparison, the fitted Nyquist plot from all 4 experiments has been plotted. For test study 2, by combination of induced 100ppm Fe^{2+} and 25ppm imidazoline, the corrosion rate obtained is the lowest as compare to others. Nevertheless, the corrosion rate resulted by injecting 50ppm imidazoline is slightly lower by difference of 0.01 (refer Table 4.5). This proven the main role of imidazoline adsorbed in the film that block the active sites on metal surface thus decrease the corrosion rate.

CHAPTER 5
CONCLUSION AND RECOMMENDATION

5.1 Conclusion

$FeCO_3$ film formation in CO_2 corrosion is due to solubility of $FeCO_3$ which depends on functions like saturation, pH and temperature. Partial $FeCO_3$ formation as produced at 80°C under natural film formation reduces corrosion rate to 0.34 mm/year. Protective film formation as produced for inducing method reduces corrosion rate down to 0.04 mm/year. This proves that protective film could reduce the corrosion rate and method to accelerate film formation could be beneficial to mitigate corrosion.

The mechanism of corrosion inhibitor adsorption is different than $FeCO_3$ film formation. Corrosion inhibitor with sufficient dosage will be able to reduce corrosion rate to a low value and $FeCO_3$ film was not present. A possible positive interaction between corrosion inhibitor and $FeCO_3$ formation could occur whereby insufficient corrosion inhibitor dosage will be supplemented by the formation of $FeCO_3$ film to reduce the corrosion rate to a low value.

5.2 Recommendations

Several parameters can be included to learn more about the mechanism and performance of $FeCO_3$ film in reducing the corrosion effect. Temperature and pH play important roles in determining the precipitation rate of iron carbonate layer. It has been said before that high pH will reduce the solubility limit of Fe^{2+} and CO_2^{3-} and increase the precipitation kinetics hence make it easier for $FeCO_3$ to precipitate. Various pH from pH 6 to pH 6.6 and temperature from 50°C to 80°C should be included in future work.

The precipitation of $FeCO_3$ is described as slow and temperature dependant process, therefore, the experiments should carry on for longer time to 48 hours or 96 hours to get a better result. The effect of multiple layers should be noticeable as longer time would increase the precipitation of $FeCO_3$ thus increase the thickness and density.

The thickness of the film formation should also been take for consideration to achieve a better result and explanation regarding the effects of density and thickness of the film towards the reduction of corrosion rate. During this test studies, the thickness of the film could not be obtained as the sample preparation before SEM is wrongly done. Instead of SEM, energy-dispersive X-ray spectroscopy (EDX) technique should be included to analyze the elements and chemical composition of the film layer. This technique is suitable in the case of test study 2 which is to observe the interaction between imidazoline and inducing Fe^{2+} ions. With EDX, determination whether $FeCO_3$ or imidazoline is dominating the composition film layer can be identified.

REFERENCES

1. A. Abid Haq , 2010, *Electrochemical Impedance Spectroscopy (EIS) Analysis of Film Formation in CO_2 Corrosion*, Thesis, Department of Mechanical Engineering, Universiti Teknologi PETRONAS.

2. J. E. Wong, N. Park, 2009, *Further Investigation on the Effect of Corrosion Inhibitor Actives on the Formation of Iron Carbonate on Carbon Steel*, Paper No. 9569, Houstan, Texas: NACE International Corrosion Conference & Expo 2009.

3. W. Sun, S. Nesic, 2006, *Kinetics of Iron Carbonate Scale Precipitation in CO_2 Corrosion*, Paper No. 6365, Houstan Texas: NACE International Corrosion Conference & Expo 2006.

4. E.Gulbrandsen, S.Nesic, A. Stangeland, T. Burchardt, *Effect of Pre-corrosion on the Performance of Inhibitor for CO2 Corrosion of Carbon Steel*, Paper No. 13, Houstan Texas: NACE International Corrosion Conference & Expo 1998.

5. K. Chokshi, W.Sun, S.Nesic, *Iron Carbonate Scale Growth & the Effect if Inhibition in CO2 Corrosion of Mild Steel*, Paper No. 05285, Houstan Texas: NACE International Corrosion Conference & Expo 2005.

6. A.Dugstad, 1998, *Mechanism of Protective Film Formation During CO2 Corrosion of Carbon Steel*, Paper No. 31, Houstan Texas: NACE International Corrosion Conference & Expo 1998.

7. V. Sridharan, 2009, *Measurement of Carbon Dioxide Corrosion on Carbon Steel using Electrochemical Frequency Modulation*, Thesis, Department of Chemical Engineering, University of Saskatchewan.

8. W. Sun, K. Chokshi, S. Nesic, D. A. Gulino, 2004, *A Study of Protective Iron Carbonate Scale Formation in CO_2 Corrosion,* Presentation Paper AIChe Annual Meeting 2004, Ohio University.

9. F. Farelas, A.Ramirez, 2010, *Carbon Dioxide Corrosion Inhibition of Carbon Steels Through Bis-imidazoline and Imidazoline Compounds Studied by EIS,* International Journal Electrochemical Science, 5 (2010) 797-814, Instituto Mexicano del Petróleo, Mexico.

10. M. B. Kermani, A. Morshed, 2003, *Carbon Dioxide Corrosion in Oil and Gas Production – A Compendium,* Corrosion Science, Vol 59, No 8.

11. H.B. Wang, H.Shi, T.Hong, C.Kang, W.P. Jepson, 2001, *Characterization of Inhibitor and Corrosion Product Film Using Electrochemical Impedance Spectroscopy (EIS),* Paper No. 1023, Houstan Texas: NACE International Corrosion Conference & Expo 2001.

12. G. Gusmano, P. Labella, G. Montesperelli, A. Privitera, S. Tassinari, 2006, *Study of the Inhibition Mecahnism of Imidazolines by Electrochemical Impedance Spectroscopy,* Corrosion Science Section Vol. 62 No. 7, July 2006, NACE International.

13. Gamry Instruments, 2007, *Application Note, Basics of Electrochemical Impedance Spectroscopy,* Gamry Instruments Copyright 2007, Rev. 5, Louis Drive Warminster, USA.

14. S. Nesic, K. L. J. Lee, V. Ruzic, 2002, *A Mechanistic Model of Iron Carbonate Film Growth and the Effect on CO2 Corrosion of Mild Steel,* Paper No. 02237, Houstan Texas: NACE International Corrosion Conference & Expo 2002.

APPENDICES

Appendix 1:

Elements	wt%
Carbon (C)	0.16
Manganese (Mn)	1.32
Phosphor (P)	0.017
Sulphur (S)	0.006
Silicon (Si)	0.31
Niobium (Nb)	0.02
Chromium (Cr)	0.01
Nickel (Ni)	0.01
Aluminium (Al)	0.03
Iron (Fe)	Balance

Appendix 2: Gantt Chart of FYP 2

TASK	DURATION	START	END	1	2	3	4	5	6	7	8	9	10	11	12	13	14	15
1	1 day	Mon (26/5/11)	Mon (26/5/11)															
2	33 days	Wed (25/5/11)	Fri (8/7/11)															
3	7 days	Mon (4/7/11)	Sun (10/7/11)															
4	1 day	Fri (15/7/11)	Fri (15/7/11)															
5	25 days	Mon (11/7/11)	Fri (12/8/11)															
6	7 days	Mon (25/8/11)	Sun (31/7/11)															
7	1 day	Fri (5/8/11)	Fri (5/8/11)															
8	11 days	Mon (1/8/11)	Thu (11/8/11)															
9	1 day	Fri (12/8/11)	Fri (12/8/11)															
10	11 days	Mon (8/8/11)	Thu (18/8/11)															
11	1 day	Fri (19/8/11)	Fri (19/8/11)															
12	7 days	Mon (15/8/11)	Sun (21/8/11)															
13	1 day	TBA	TBA															
14	7 days	Mon (22/8/11)	Sun (28/8/11)															
15	1 day	Fri (2/9/11)	Fri (2/9/11)															

1 : FYP 2 Briefing

2 : Project work continues

3 : Progress report preparation

4 : Submission of progress report

5 : Project work continues

6 : Pre-EDX preparation

7 : Pre-EDX

8 : Draft report preparation

9 : Submission of draft report

10 : Technical paper and dissertation (soft bound) preparation

11 : Submission of technical paper and dissertation (soft bound)

12 : Oral presentation preparation

13 : Oral presentation

14 : Dissertation (hard bound) preparation

15 : Submission of dissertation (hardbound)